

Metalurško tehnološki fakultet

Vijeću

Broj 2237
Podgorica, 11. 10 2023 god.

Predmet: Saglasnost za nastavak procedure za MSc Zoranu Sekulić, studentkinju doktorskih studija

U skladu sa članom 31a, **Pravila o izmjenama i dopunama pravila doktorskih studija (Bilten UCG br.561, od 4.07.2022)**, mentorka prof. dr Vanja Asanović je Komisiji za doktorske studije MTF-a, podnijela izvještaj o radu studentkinje doktorskih studija MSc Zorane Sekulić, a koji se odnosi na sprovedena istraživanja i postignute rezultate u studijskoj 2022/23. godini.

Komisija je izvršila uvid u obrazloženje mentorke o sprovedenim istraživanjima i publikovanim radovima u protekloj studijskoj godini. Konstatovano je da doktorandkinja ima 2 rada u časopisima sa SCI/SCIE liste, od kojih je jedan publikovan, a drugi prihvaćen za publikovanje i dostupan on line.

Rezultati koje je doktorandkinja postigla u prethodnoj studijskoj godini, detaljno su objašnjeni od strane mentorke, na osnovu čega je konstatovano da je doktorandkinja ostvarila napredak prema predviđenom planu rada na tezi.

Na osnovu uvida u priložene radove i ocjene mentorke da kandidatkinja može nastaviti sa radom na istraživanjima, Komisija smatra da je doktorandkinja uspješno završila prethodnu studijsku godinu i predlaže nastavak daljih istraživanja u skladu sa istraživačkim planom.

Podgorica, Oktobra 2023

Komisija

Prof. dr Mira Vukčević

Prof. dr Zorica Leka

Prof. dr Ivana Bošković

UNIVERZITET CRNE GORE Broj. 2203
Podgorica, 09.10.23 god.
METALURŠKO-TEHNOLOŠKI FAKULTET

Podgorica

PREDMET: Godišnji izvještaj mentora o napredovanju doktoranda

Poštovani,

U skladu sa Pravilima o izmjenama i dopunama pravila doktorskih studija (Bilten Univerziteta Crne Gore, br. 561 od 04.07.2022. godine), dostavljam Vam Godišnji izvještaj mentora o napredovanju doktoranda MSc Zorane Sekulić.

Srdačan pozdrav,

Mentor



Prof. dr Vanja Asanović

Podgorica, 09.10.2023.g.

GODIŠNJI IZVJEŠTAJ MENTORA O NAPREDOVANJU DOKTORANDA

Akademska godina za koju se podnosi izvještaj		2022/2023	
OPŠTI PODACI O DOKTORANDU			
Titula, ime, ime roditelja, prezime	MSc Zorana Sekulić		
Fakultet	Metalurško-tehnološki fakultet		
Studijski program	Metalurgija i materijali		
Broj indeksa	1/19		
MENTOR/MENTORI			
Mentor	Prof. dr Vanja Asanović	UCG, Crna Gora	Fizička metalurgija
Ko-mentor	Dr Jasmina Grbović Novaković	Institut za nuklerane nauke „Vinča“, Institut od nacionalnog značaja za Republiku Srbiju, Republika Srbija	Fizička hemija materijala
EVALUACIJA DOKTORANDA*			
Koliko ste zadovoljni kvalitetom održanih susreta sa doktorandom?	<input type="checkbox"/> 1 <input type="checkbox"/> 2 <input type="checkbox"/> 3 <input type="checkbox"/> 4 <input checked="" type="checkbox"/> 5		
(Ako je prethodni odgovor „1“ ili „2“ dati obrazloženje i prijedloge za poboljšanje)			
Da li je definisan plan rada sa doktorandom?	<input checked="" type="checkbox"/> DA <input type="checkbox"/> NE		
Da li je doktorand ostvario napredak prema predviđenom planu rada?	<input checked="" type="checkbox"/> DA <input type="checkbox"/> NE		
(Ako je prethodni odgovor „ne“ dati obrazloženje i prijedloge za poboljšanje)			
Kvalitet napretka doktorandovog istraživačkog rada u periodu za koji se podnosi izvještaj je:	<input type="checkbox"/> 1 <input type="checkbox"/> 2 <input type="checkbox"/> 3 <input type="checkbox"/> 4 <input checked="" type="checkbox"/> 5		
(Ako je prethodni odgovor „1“ ili „2“ dati obrazloženje i prijedloge za poboljšanje)			
Ocjena doktorandove spremnosti za konsultacije.	<input type="checkbox"/> 1 <input type="checkbox"/> 2 <input type="checkbox"/> 3 <input type="checkbox"/> 4 <input checked="" type="checkbox"/> 5		
Ocjena planiranja i izvršavanja godišnjih istraživačkih aktivnosti i stručnog usavršavanja doktoranda.	<input type="checkbox"/> 1 <input type="checkbox"/> 2 <input type="checkbox"/> 3 <input type="checkbox"/> 4 <input checked="" type="checkbox"/> 5		
Ocjena napretka u savladavanju metodologije naučno-istraživačkog rada.	<input type="checkbox"/> 1 <input type="checkbox"/> 2 <input type="checkbox"/> 3 <input type="checkbox"/> 4 <input checked="" type="checkbox"/> 5		
Ocjena doktorandovog generalnog odnosa prema studijama.	<input type="checkbox"/> 1 <input type="checkbox"/> 2 <input type="checkbox"/> 3 <input type="checkbox"/> 4 <input checked="" type="checkbox"/> 5		
Ocjena ukupnog kvaliteta doktorandovog rada.	<input type="checkbox"/> 1 <input type="checkbox"/> 2 <input type="checkbox"/> 3 <input type="checkbox"/> 4 <input checked="" type="checkbox"/> 5		
(Ako je prethodni odgovor „1“ ili „2“ dati obrazloženje i prijedloge za poboljšanje)			

*Ocjene su: 1 – nedovoljan, 2 – dovoljan, 3 – dobar, 4 – vrlo dobar, 5 – odličan

ISPUNJENOST USLOVA DOKTORANDA
<p>Spisak radova doktoranda iz oblasti doktorskih studija koje je publikovao doktorand (dati spisak radova koji sadrži)</p> <p>Doktorantkinja MSc Zorana Sekulić je rezultate sprovedenog istraživanja predstavila u sljedećim radovima koji su objavljeni u naučnim časopisima za sa SCI/SCIE liste:</p> <ol style="list-style-type: none"> 1. Babić B., Prvulović M., Filipović N., Mravik Ž., Sekulić Z., Milošević Govedarović S., Milanović I., "Hydrogen storage properties of MgH_2-Tm: Ni-catalysis vs. mechanical milling", <i>International Journal of Hydrogen Energy</i>, 2023, SSN 0360-3199, Article in press, Available online 26 April 2023, https://doi.org/10.1016/j.ijhydene.2023.04.078, (https://www.sciencedirect.com/science/article/pii/S036031992301813X). 2. Sekulić Z., Grbović Novaković J., Babić B., Prvulović M., Milanović I., Novaković N., Rajnović D., Filipović N., Asanović V., "The Catalytic Effect of Vanadium on Sorption Properties of MgH_2-Based Nanocomposites Obtained Using Low Milling Time, <i>Materials</i>, 2023, 16, 5480. https://doi.org/10.3390/ma16155480.
<p>Obrazloženje mentora o korišćenju sprovedenih istraživanja u publikovanim radovima (dati obrazloženje)</p> <p>Planom istraživanja predviđeno je proučavanje faznih transformacija, ispitivanje strukture i kristalne strukture, istraživanje katalitičkog efekta 3d, 4d i 5d metala na sorpcionu kinetiku vodonika u nanokompozitnom materijalu, kao i uticaja na termodinamičku stabilnost magnezijum hidrida, MgH_2.</p> <p>U radu <i>Hydrogen storage properties of MgH_2-Tm: Ni-catalysis vs. mechanical milling</i>?, predstavljeni su rezultati istraživanja uticaja dodavanja nikla na desorpciju vodonika iz kompozita MgH_2-Ni. Kompozitni prah je mljeven 15 min, 30 min i 45 min, a za karakterizaciju kompozita su primijenjene: rendgenska difrakciona analiza (XRD), skenirajuća elektronska mikroskopija sa energetski disperzivnom spektrometrijom (SEM-EDS), laserska metoda za određivanje raspodjele veličine čestica (PSD), diferencijalna skenirajuća kalorimetrija (DSC) i temperaturno programirana desorpcija (TPD). Primijećeno je da ravnomjerna raspodjela utiče na snižavanje temperature desorpcije vodonika za više od 100 °C. Utvrđeno je da se reakcija desorpcije vodonika u katalizovanim uzorcima može opisati kinetičkim mehanizmom Avrami-Erofejeva (Avrami-Erofeev) sa vrijednošću parametra $n = 4$. Prividna energija aktivacije reakcije desorpcije vodonika se smanjivala sa povećanjem vremena mljevenja i dodatkom nikla. Ovo istraživanje je po prvi put pokazalo da se dva glavna procesa (mljevenje i katalitičko djelovanje) mogu zasebno analizirati. Zaključeno je da u toku kratkotrajnih vremena mljevenja, prevladuje katalitički efekat nikla.</p> <p>U radu <i>The Catalytic Effect of Vanadium on Sorption Properties of MgH_2-Based Nanocomposites Obtained Using Low Milling Time</i>, prikazani su rezultati analize uticaja katalitičkog efekta vanadijuma na desorpcione karakteristike kompozita. Primjenom mehanohemijskog mljevenja u visokoenergetskom kugličnom mlinu, kao metode zelene sinteze u inertnoj atmosferi argona, sintetizovan je kompozit magnezijum hidrid-vanadijum. Odnos mase kuglica i mase praha upotrijebljenog materijala BPR (Ball to Powder Ratio) iznosio je $\approx 10:1$, a mljevenje magnezijum hidrida sa dodatkom vanadijuma u količini od 2 mas % i 5 mas % je realizovano pri različitim vremenskim intervalima od 15 min do 45 min. Mikrostrukturalna istraživanja su sprovedena primjenom rendgenske difrakcione analize (XRD) i infracrvene spektroskopije sa Furijeovom</p>

transformacijom, morfologija je ispitivana pomoću skenirajuće elektronske mikroskopije (SEM), a utvrđena je i raspodjela čestica na osnovu njihove veličine (laserska difrakcija za analizu veličine čestica - PSD). Termičke promjene su istraživane pomoću diferencijalne skenirajuće kalorimetrije (DSC) i temperaturno programirane desorpcija (TPD).

Utvrđeno je da se temperatura desorpcije vodonika snižava u prisustvu dopanta za nekoliko desetina stepeni usljed katalitičkog dejstva vanadijuma. U pogledu temperature desorpcije i prividne energije aktivacije, najbolji rezultati se očekuju za uzorak koji je mljeven 30 min, pri sadržaju aditiva of 5 mas %. Istraživanje je pokazalo da se veličina čestica značajno smanjuje čak i pri mljevenju u toku kraćih vremenskih intervala, a da se raspodjela veličine čestica mijenja od monomodalne raspodjele karakteristične za nemljeveni MgH_2 do polimodalne raspodjele karakteristične za kompozite dobijene mljevenjem u toku 30 min. Primijećena desorpcija H_2 na niskoj temperaturi se može pripisati manjoj veličini čestica MgH_2 . Utvrđeno je da kratka vremena mljevenja odgovaraju prividnim energijama aktivacije od 70 kJ/mol, a da dodavanje vanadijuma ne utiče značajno na temperaturu desorpcije.

Ocjena o aktivnostima sprovedenim na pisanju i objavljivanju naučnih radova.

☐ 1 ☐ 2 ☐ 3 ☐ 4 ☒ 5

SAGLASNOST ZA NASTAVAK STUDIJA

Može li doktorand nastaviti studije?

☒ Da
☐ Da, uz određene uslove
☐ Ne

(Ako je prethodno dat odgovor pod „Da, uz određene uslove“ ili „Ne“ dati obrazloženje i prijedloge za poboljšanje)

Napomene

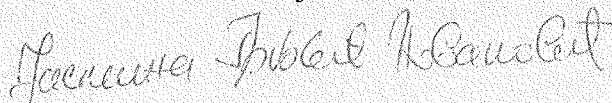
(Popuniti po potrebi)

U Podgorici,
06.10.2023.

Prof. dr Vanja Asanović



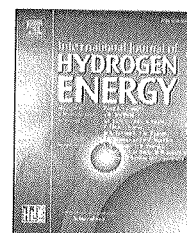
dr Jasmina Grbović Novaković



MP

Prilog dokumenta sadrži:

- Objavljeni rezultati rada na izradi doktorske disertacije (za drugi izvještaj mentora)



Hydrogen storage properties of $\text{MgH}_2\text{--Tm}$: Ni-catalysis vs. mechanical milling

Bojana Babić^a, Milica Prvulović^a, Nenad Filipović^b, Željko Mravik^a,
Zorana Sekulić^c, Sanja Milošević Govedarović^a, Igor Milanović^{a,*}

^a Vinča Institute of Nuclear Sciences, National Institute of the Republic of Serbia, Centre of Excellence for Renewable and Hydrogen Energy, University of Belgrade, POB 522, 11000 Belgrade, Serbia

^b Institute of Technical Sciences of SASA, Knez Mihajlova 35/IV, 11000 Belgrade, Serbia

^c Ministry of Capital Investments, The Government of Montenegro, Directorate for Energy and Energy Efficiency, Rimski Trg 46, 81 000 Podgorica, Montenegro

HIGHLIGHTS

- For the first time two main processes grinding and catalytic effect are separately analyzed in $\text{MgH}_2\text{--Ni}$ solid state system.
- Milling itself does not induce significant particle size reduction (for investigated milling times).
- Milling process leads only to mixing of MgH_2 and Ni powders for milling times up to 45 min.
- Mechanical milling of $\text{MgH}_2\text{--Ni}$ solid state system leads to better distribution of Ni particles in MgH_2 bulk.
- For investigated milling times only catalytic effect of Ni is dominant.

ARTICLE INFO

Article history:

Received 25 January 2023

Received in revised form

9 March 2023

Accepted 6 April 2023

Available online xxx

Keywords:

Ni-catalysis of H_2 desorption

Mechanochemistry

Ball milling

$\text{MgH}_2\text{--Ni}$ system

Hydrogen desorption temperature

Hydrogen storage of MgH_2 based system

ABSTRACT

The influence of the addition of nickel on hydrogen desorption from the $\text{MgH}_2\text{--Ni}$ composite was investigated. The composite powder was ball-milled for 15, 30 and 45 min and characterized by XRD, SEM-EDS, PSD, DSC and TPD methods. It was observed that the uniform distribution of nickel decreases hydrogen desorption temperature by more than 100 °C. A kinetic model for the hydrogen desorption process was also determined. The hydrogen desorption reaction in catalyzed samples is described by the Avrami-Erofeev model with the value of parameter $n = 4$. The apparent activation energy of the hydrogen desorption reaction was decreased with the increase of milling time and the addition of nickel. It has been shown for the first time that two main processes (grinding and the catalytic effect) could be separately analyzed. It is concluded that for investigated short milling times, the catalytic effect of Ni is predominant.

© 2023 Hydrogen Energy Publications LLC. Published by Elsevier Ltd. All rights reserved.

* Corresponding author. Vinča Institute of Nuclear Sciences, National Institute of the Republic of Serbia, Centre of Excellence for Renewable and Hydrogen Energy, University of Belgrade, P.O. Box 522, 11000 Belgrade, Serbia.

E-mail address: igorm@vin.bg.ac.rs (I. Milanović).

<https://doi.org/10.1016/j.ijhydene.2023.04.078>

0360-3199/© 2023 Hydrogen Energy Publications LLC. Published by Elsevier Ltd. All rights reserved.

Introduction

Nowadays there is a great demand for renewable energy sources. Hydrogen, as one of the possible solutions has a lot of advantages in comparison to fossil fuels: oxidation in fuel cells with an absence of CO₂ emission [1], supports a circular and environmentally friendly economy [2], abundance (practically unlimited quantities if produced from water) etc. The most important advantage is that the usage of hydrogen in fuel cells produces electrical current as a product and water as a byproduct which makes this process safe for the environment. In respect to the application proposes, among of three storage possibilities: gaseous, liquid and solid-state storage, only storage in solid medium meets the requirement of H₂ density [2,3] (same as in the petrol tanks). Metal hydrides possess characteristics such as high volumetric density of hydrogen, high gravimetric capacity of hydrogen, good kinetics and cyclic behavior, low toxicity, low working pressure of H₂ and safety but also several drawbacks: sluggish kinetics, high desorption temperature and low thermal conductivities of pure hydrides [4].

The most investigated hydride in the last 20 years is magnesium hydride (MgH₂) because of its low cost and high gravimetric capacity [4–6]. Its modification conceives better conditions for hydrogen storage [7–10]. This can be achieved by changing the microstructure of the hydride either by mechanical milling with additives [11–17], which reduces the stability of the hydride [4,11–17] or by ion irradiation [7,9]. By using the small quantities of additives (up to 10 wt%), the hydrogen storage capacity of starting hydride remains practically unchanged. As additives, metals, metal oxides and intermetallic compounds were used [4,13,18–20]. The addition of transition metals (Tm) improves hydrogen storage properties because of their simultaneous catalytic effect on sorption processes. The commonly used metals as a catalyst are nickel (Ni) [17,21–34], titanium (Ti) [11,16,20,21,28,35,36], vanadium (V) [16,21,28,37], manganese (Mn) [21], iron (Fe) [21,38], copper (Cu) [21], cobalt (Co) [21], palladium (Pd) [21] and niobium (Nb) [11,16,21,22,28,35,37,39]. Liang et al. [28] have investigated MgH₂ – Tm (Ti, V, Mn, Fe, Ni) nanocomposites prepared by mechanical milling MgH₂ with 5 at.% of Tm within 20 h. The system MgH₂ + 5 at.% Ti showed the fastest desorption kinetic of hydrogen at 300 °C and 250 °C. The activation energy of this system is 71.1 kJ/mol. It is shown that MgH₂ + 5 at.% V can desorb hydrogen completely under vacuum within 2000 s at 300 °C and 900 s at 250 °C. Liang et al. obtained the apparent activation energy of 62 kJ/mol for the MgH₂ + 5 at.% V system, which is twice as less than the activation energy of pure MgH₂ (120 kJ/mol) [28]. The sorption of composite MgH₂ + 5 at.% V also has been examined during 2000 cycles at 300 °C [37] by Z. Dehouche and co-workers, who concluded that the system remains stable without of reduction in kinetic rates. The lower temperature of hydrogen desorption is noticed in composite MgH₂ + 5 at.% Ti milled for 2 h. For as-received MgH₂ desorption temperature is 422 °C and for this system 370 °C. On the other hand, composite MgH₂ with 2 mol% Ni milled for 2 h at 250 °C absorbed 5.3 wt% hydrogen for only 5 min [23]. Also, next papers confirm the outstanding properties of nickel as a catalyst. Huot and co-workers investigated the presence

of nickel reduced the onset temperature of decomposition from 440.7 °C to 225.4 °C [29]. The MgH₂–Ni composite shows better kinetics when compared to the MgH₂–Ni alloy because the composite has a 10 times larger specific surface area then the alloy [28]. El-Eskandarany et al. examined MgH₂ catalyzed with Ni nanograins, which have enormous benefits for increasing the kinetics of hydrogenation/dehydrogenation at 275 °C. The powders milled for 25 h desorbs H₂ after only 2.5 min and absorb H₂ in 8 min, unlike MgH₂ which shows very slow kinetics at temperatures lower than 350 °C [30]. Gao et al. [24] investigated MgH₂ + 7 wt% NiV-based two dimensional layered double hydroxide and they found that the initial desorption temperature of MgH₂ was significantly reduced to 190 °C. It has been concluded that the homogeneous dispersion and unique heterostructure of Mg₂Ni/Mg₂NiH₄ and metallic V, cooperated to provide more reaction sites and diffusion paths, enabling enhanced hydrogen storage performance of MgH₂. Hu et al. [25] investigated the system MgH₂ + 10 wt% TiMgVNi₃. They found that the particle size and distribution of catalytic phases, (Ti, V)H₂ and Mg₂Ni are the key factor for MgH₂ hydrogen desorption kinetics also. Importance of Mg₂Ni is also confirmed by other authors [26,31]. Tan et al. investigated Mg–Ni–TiS₂ composites and found that improved hydrogen desorption kinetics is attributed to synergistical catalytic effect of the Mg₂NiH₄ and TiH₂, both formed during the first absorption cycle [26].

In the present work, we have studied the catalytic effect of Ni particles milled with MgH₂ powder and their effect on hydrogen desorption properties. The goal of our research was to investigate which of two effects is more dominant in MgH₂ – Ni system: i) catalytic influence of added metal or ii) grinding effect of milling. According to our best knowledge, there are no comparative studies of these two effects on the hydrogen desorption properties.

Experimental

Pure MgH₂ (Langfang Great AP Chemicals Co, purity 98%) and system MgH₂ with 5 wt% of nickel (Johnson Matthey Alfa Products, purity 99.99%) – powders were milled for different milling times – 15, 30, and 45 min. To prevent the oxidation of the sample, the experiments were done in an inert argon atmosphere. For this purpose we have used SPEX 5100 mixer/mill (2500 RPM). The grinding vessel was made of stainless steel as well as balls. The ball to powder ratio was ≈16:1.

Phase structures of the ball-milled powders were characterized by X-ray diffraction (XRD) on Rigaku Ultima IV diffractometer using a nickel filter and Cu-Kα radiation (λ = 0.1540 nm), in the 2θ range between 10° and 90°, at operating parameters of 40 kV and 40 mA. The presented XRD measurements were made with a step of 0.02° and the accumulative time was 5 s at every point.

The distribution of particles based on their size was analyzed using Mastersizer 2000, Malvern instruments Ltd. UK which measures particle size in the range of 0.02–2000 μm using He-Ne laser (λ = 633 nm). The samples were dispersed in isopropanol and after that placed in an ultrasonic bath for 5 min to avoid agglomeration.

The micrographs are obtained by Scanning Electron Microscope (SEM) JEOL JSM 6460LV and Oxford Instrument INCA-X-sight.

The thermal properties of the milled powders were measured by the DSC apparatus SETARAM DSC 131 Evo. The accurately measured samples (between 3 and 5 mg) were placed in Al measuring vessels and sealed with the lids. The samples were further subjected to a heating regime from room temperature to 530 °C, with a heating rate of 5 °C/min.

Temperature programmed desorption (TPD) was used for the analysis of desorption products during the heating. About 0.6 mg of sample was placed in a quartz cuvette. After the system is evacuated to about 1×10^{-7} mbar, the cuvette is heated at a rate of 10 °C/min from room temperature to 513 °C. The analysis of desorbed gases was carried out on a mass spectrometer Extorr 300 with five mass to charge ratio (m/z): 1 (H), 2 (H₂), 17 (OH), 18 (H₂O), and 28 (N₂ and CO).

Results and discussion

Fig. 1 shows a diffractograms of MgH₂ milled for 15, 30, and 45 min compared to the diffractogram of as-received (commercial) MgH₂. Based on the position of characteristic diffraction maxima, the presence of β -MgH₂ is dominant. Also, the presence of γ -MgH₂ phase is occurring in samples with a milling time longer than 15 min. The intensity of the

diffraction maxima is increasing with milling time, i.e. the amount of γ -MgH₂ grows, while broadening of β -MgH₂ phase diffraction maxima is evident (decrease in crystallite size). In comparison to as-received MgH₂ (which has only β -MgH₂) milled MgH₂ has broader maxima. Fig. 2 shows diffractograms of MgH₂ samples with 5 wt% Ni milled for 15, 30, and 45 min in comparison with the diffractogram of as-received (commercial) MgH₂. Three additional maxima (marked with "o" in Fig. 2 b-d) are originating from the presence of nickel [13]. By comparing the samples with (Fig. 2) and without Ni (Fig. 1), changes in phase composition during the milling process are not noticed (Table 1). This means that Ni powder does not affect the milling process. In Table 1 the positions of maxima for γ -MgH₂ and the nickel phase are listed.

The particle size distribution (PSD) of samples is shown in Fig. 3. As-received MgH₂ shows a monomodal particle size distribution with maximum of 26 μ m. On the other hand, all milled MgH₂ samples show bimodal particle size distribution. These samples have a significantly wider range of distribution predominantly at the lower values. The decrease in particle size was noticed for a longer milling time. Table 2 shows the values of particle size range and average particle size.

Fig. 4 shows the distribution of particle sizes for as-received MgH₂ and milled MgH₂ + 5 wt% Ni samples. All the MgH₂ + 5 wt% Ni samples have bimodal particle distribution.

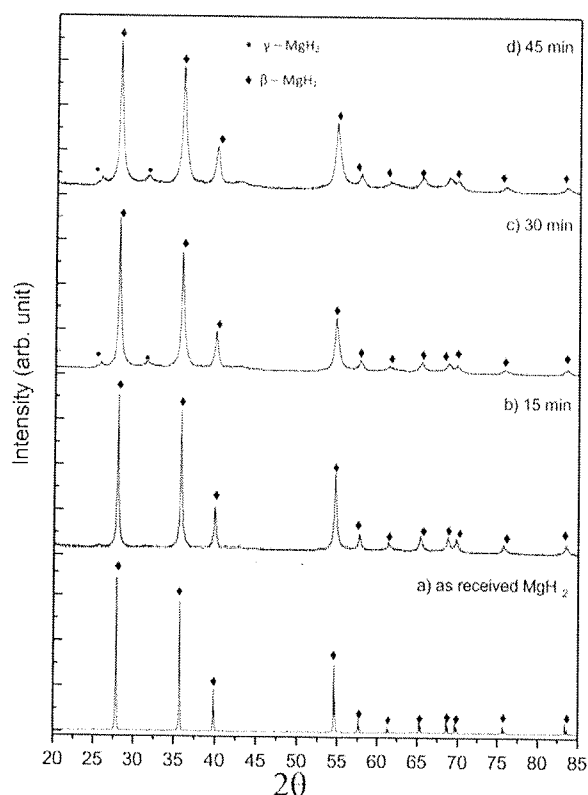


Fig. 1 – Diffractograms of as-received and milled MgH₂: a) as-received MgH₂; b) MgH₂ milled for 15 min; c) MgH₂ milled for 30 min; d) MgH₂ milled for 45 min.

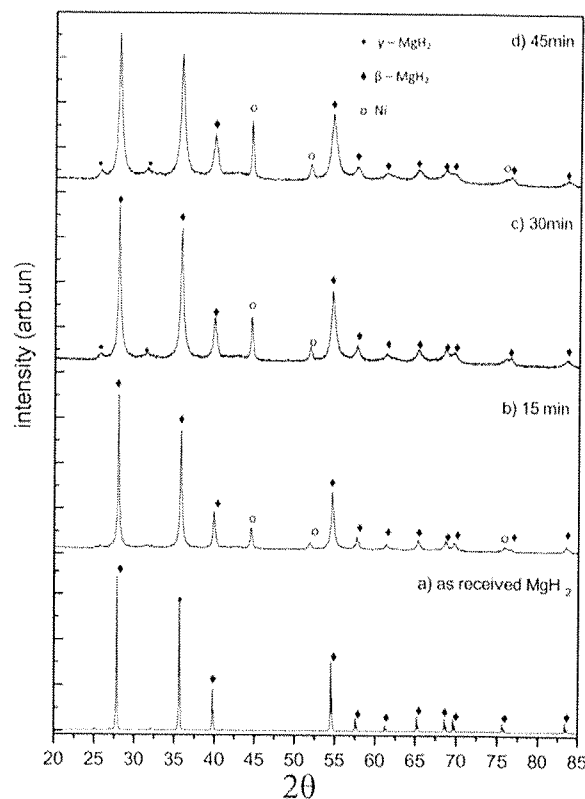
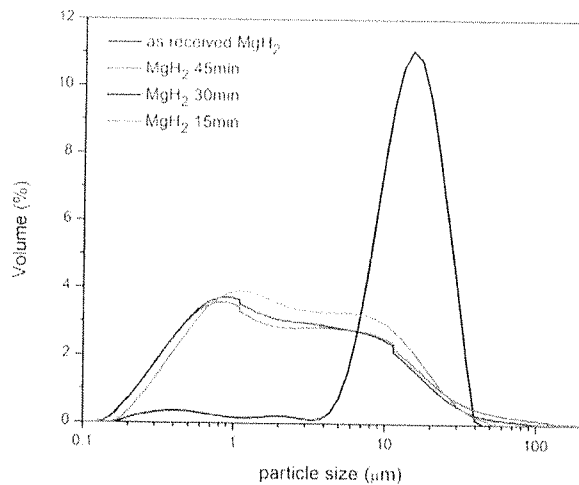
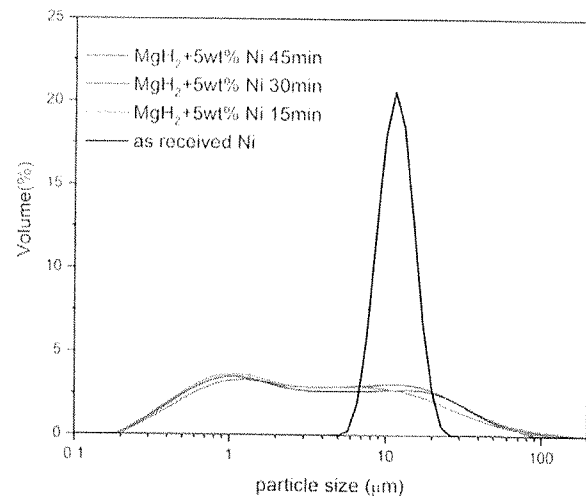


Fig. 2 – Diffractograms of as-received MgH₂ and milled MgH₂ + 5 wt% Ni: a) as-received MgH₂; b) MgH₂ + 5 wt% Ni milled for 15 min; c) MgH₂ + 5 wt% Ni milled for 30 min; d) MgH₂ + 5 wt% Ni milled for 45 min.

Table 1 – Position of maxima for γ – MgH_2 and Ni phase on diffractograms obtained by XRD analysis of MgH_2 sample and $\text{MgH}_2 + 5 \text{ wt\% Ni}$ sample milled for 15, 30, and 45 min.

Sample	MgH_2 15 min	MgH_2 30 min	MgH_2 45 min	$\text{MgH}_2 + 5 \text{ wt\% Ni}$ 15 min	$\text{MgH}_2 + 5 \text{ wt\% Ni}$ 30 min	$\text{MgH}_2 + 5 \text{ wt\% Ni}$ 45 min
γ – MgH_2	/	54.71°(20)	27.86°(20)	/	25.71°(20)	44.53°(20)
Ni	/	39.89°(20)	35.80°(20)	/	31.53°(20)	51.81°(20)
	/	/	/	44.64°(20)	44.53°(20)	44.64°(20)
	/	/	/	51.88°(20)	51.81°(20)	51.92°(20)
	/	/	/	76.04°(20)	76.33°(20)	76.48°(20)

**Fig. 3 – Particle size distribution (PSD) of as-received MgH_2 and milled for 15, 30, and 45 min.****Fig. 4 – Particle size distribution (PSD) of as-received Ni, and $\text{MgH}_2 + 5 \text{ wt\% Ni}$ samples milled for 15, 30, and 45 min.**

As the milling time increases, the medium particle size remains approximately the same or minimally increased due to agglomeration. Compared to the samples without the addition of nickel, the obtained average particle sizes (see Table 2), as well as distribution widths, are slightly higher (except in the case of pure MgH_2 milled for 45 min which has a wider distribution range than the samples with the addition of nickel).

It is concluded that the presence of additives has little effect on the particle size distribution (see Fig. 4). Also, the distribution of particle size analysis of all MgH_2 –Ni samples

shows that there is no significant dependence of particle size distribution and milling time (see Figs. 3 and 4).

The morphology of samples is presented by micrographs in Fig. 5. Particles of as-received MgH_2 powder (Fig. 5a) possess very characteristic globular MgH_2 particles and hexagonal Mg particles in the range between several to 25 μm . Sample $\text{MgH}_2 + 5 \text{ wt\% Ni}$ milled for 15 min (Fig. 5b) shows the presence of irregular sponge-like particles, with dimensions from several microns to 40 μm . The increase of average particle size and

Table 2 – The values of particle size range and average particle size obtained by PSD.

Sample	Particle size range (μm)	Average particle size (μm)
As-received MgH_2	0.7–70	26
MgH_2 15 min	0.1–3.5	1.1
	3.5–59	5.5
MgH_2 30 min	0.1–2.1	0.9
	2.1–115	5.1
MgH_2 45 min	0.1–2.4	0.8
	2.4–208	4.1
$\text{MgH}_2 + 5 \text{ wt\% Ni}$ 15min	0.2–3.7	1.1
	3.7–141	6.4
$\text{MgH}_2 + 5 \text{ wt\% Ni}$ 30min	0.2–4.9	1.1
	4.8–187	13.2
$\text{MgH}_2 + 5 \text{ wt\% Ni}$ 45min	0.2–3.8	1.2
	3.8–100	11.7

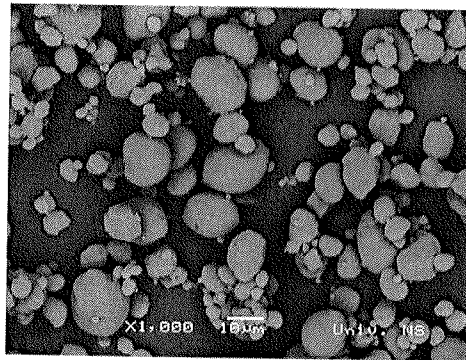
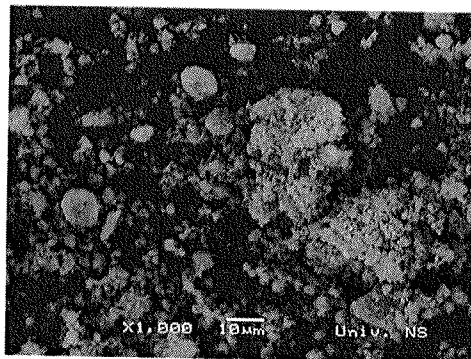
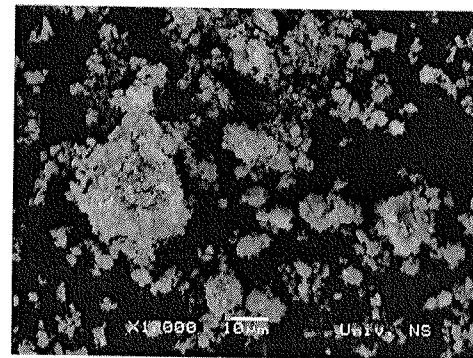
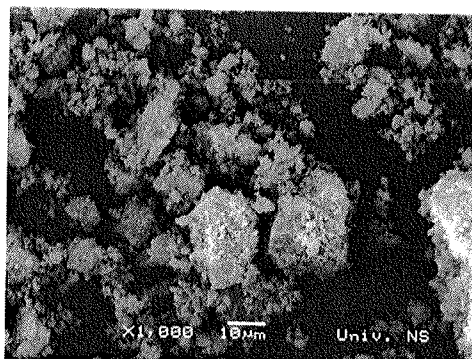
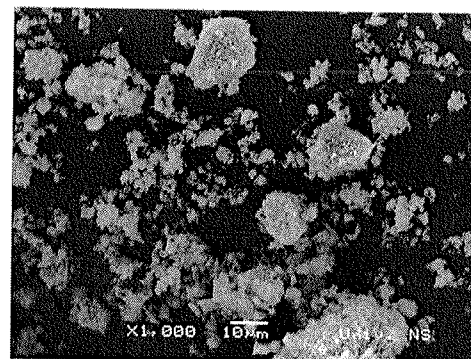
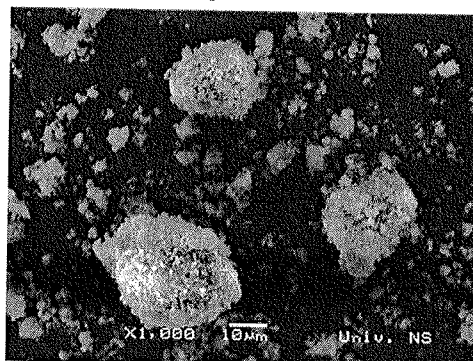
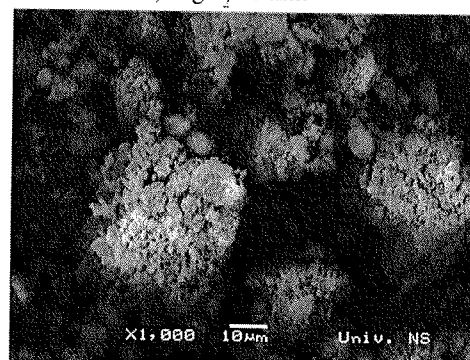
a) as-received MgH_2 b) $\text{MgH}_2\text{-Ni}$ 15 minc) MgH_2 15 minc) $\text{MgH}_2\text{-Ni}$ 30 minf) MgH_2 30 mind) $\text{MgH}_2\text{-Ni}$ 45 ming) MgH_2 45 min

Fig. 5 – SEM micrographs of as-received MgH_2 (a), milled $\text{MgH}_2\text{-Ni}$ (b, c, d) and milled pure MgH_2 (e, f, g).

formation of larger agglomerates are visible in sample $\text{MgH}_2 + 5 \text{ wt\% Ni}$ milled for 30 min (Fig. 5b). If the milling time increases to 45 min the predominantly irregularly shaped agglomerates with sizes between 20 and 50 μm are formed. To compare results obtained with $\text{MgH}_2 + 5 \text{ wt\% Ni}$ system, as-received MgH_2 was also milled for 15, 30 and 45 min. As shown in Fig. 5e, f and g, shape and dimensions of particles in milled MgH_2 are very similar in comparison with $\text{MgH}_2 + 5 \text{ wt\% Ni}$ samples. This fact indicates that nickel does not act as a milling agent in particle size reduction, and therefore has no influence on the morphology. Previous studies have demonstrated that incorporating Ni as an additive during the milling process of MgH_2 does not significantly impact the particle size of the material [40–42]. Additionally, increasing the concentration of Ni additive does not affect the particle size of MgH_2 [39].

To investigate the dispersion of Ni particles in MgH_2 all the samples with nickel are measured with SEM-EDS analysis. The EDS analysis and micrographs are shown in Fig. 6. From the SEM image of $\text{MgH}_2 + 5 \text{ wt\% Ni}$ milled for 15 min (Fig. 6a) and its EDS profile it is obvious that round nickel particle stayed unmilled and captured in MgH_2 powder. EDS maps of nickel and magnesium prove that the dispersion of round nickel particles is very weak in magnesium hydride powder. From the SEM-EDS micrographs (Fig. 6 a and b), in the samples

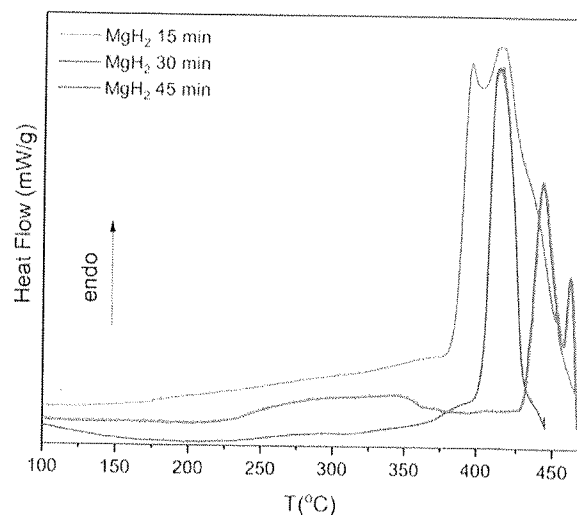


Fig. 7 – DSC curves of MgH_2 milled for 15, 30 and 45 min.

$\text{MgH}_2 + 5 \text{ wt\% Ni}$ milled for 15 min and $\text{MgH}_2 + 5 \text{ wt\% Ni}$ milled for 30 min, the particle of round-shaped Ni particles are clearly visible and their size correspond to the values obtained from PSD of as received Ni (around 10 μm , Fig. 4). Finally, the

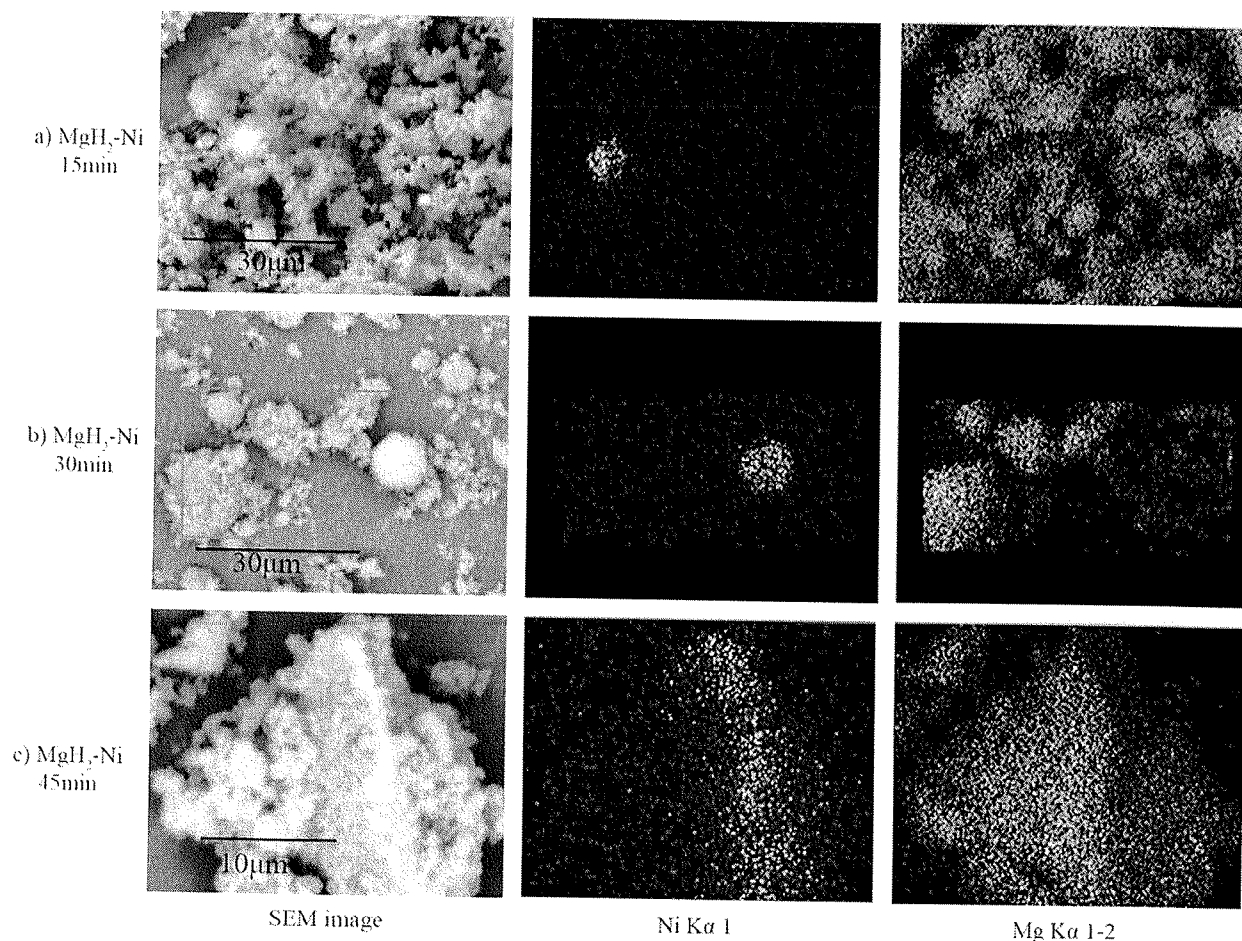


Fig. 6 – SEM-EDS micrographs of milled MgH_2 -Ni composite.

most significant changes are noticed in $\text{MgH}_2 + 5 \text{ wt\% Ni}$ sample milled for 45 min (Fig. 6c). Globular nickel particles in sample milled for 45 min are reduced to very small nanometric particles which very easily penetrate in MgH_2 bulk. As a result, complete quantity of nickel powder is mixed with MgH_2 particles. The research conducted by Xie et al. [22] found that a more uniform distribution of nickel on the surface of MgH_2 improves the kinetics of the dehydrogenation reaction. In the samples with weak dispersion of Ni particles, hydrogen desorption properties (DSC and TPD) are quite the same as in pure MgH_2 milled during the same period. On the other hand, a sample with a very good distribution of Ni particles (milled for 45 min) shows much better H_2 desorption behavior. This can be attributed to the beneficial effect of the Ni on the hydrogen recombination reaction. The findings of this paper, which confirm the positive impact of an uniform distribution of nickel on the catalytic dehydrogenation reaction, align with previously published results [21,22,30,39,40].

The DSC curves of MgH_2 milled for 15, 30 and 45 min are shown in Fig. 7. The endothermic maxima are visible for all samples. Two desorption maxima at temperatures 396 °C and 416 °C are visible for MgH_2 milled for 15 min. The sample milled for 30 min have two maxima: shoulder at 375 °C and maximum at 414 °C. In the case of MgH_2 milled for 45 min, three maxima are visible: in a range of 218 °C–361 °C which belongs to hydrogen released from $\gamma - \text{MgH}_2$ [30], and two maxima originating from $\beta - \text{MgH}_2$ at 444 °C and 462 °C. With the increase in milling time, the temperature of desorption hydrogen from MgH_2 also increases. This behavior is a consequence of the agglomeration of MgH_2 particles, which is confirmed by SEM images (Figs. 5 and 6). The shorter milling time has a better influence on the properties of pure MgH_2 [43].

Fig. 8 shows DSC curves of MgH_2 with the addition of 5 wt% Ni milled for 15, 30 and 45 min. Sample $\text{MgH}_2 + 5 \text{ wt\% Ni}$ milled for 15 min, desorbs hydrogen at 376 °C and 415 °C. For $\text{MgH}_2 + 5 \text{ wt\% Ni}$ milled for 30 min, maxima occurs at temperatures 376 °C and 428 °C. The lowest desorption temperature (360 °C) appears in the sample milled for 45 min and the

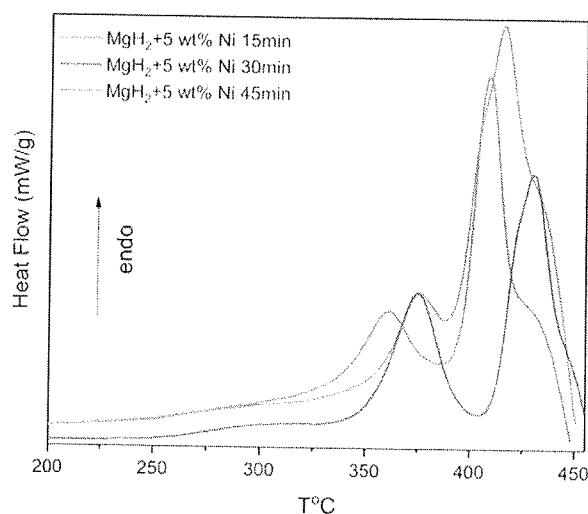


Fig. 8 – DSC curves of $\text{MgH}_2 + 5 \text{ wt\% Ni}$ milled for 15, 30 and 45 min.

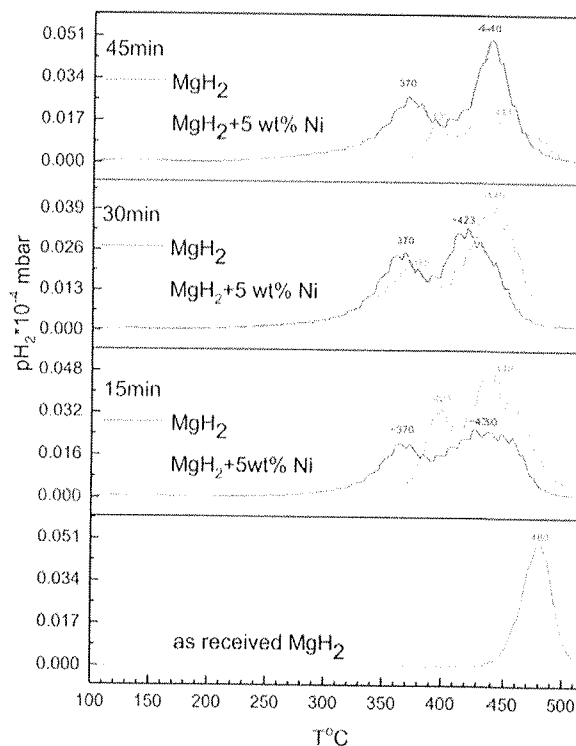


Fig. 9 – Temperature programmed desorption (TPD) profiles of as-received MgH_2 (blue line), milled MgH_2 (red line), and milled $\text{MgH}_2 + 5 \text{ wt\% Ni}$ (black line). (For interpretation of the references to color in this figure legend, the reader is referred to the Web version of this article.)

second maximum appears at 410 °C. Shoulder in the range of 275–325 °C, analogue to the sample MgH_2 milled for 45min, also originates from $\gamma - \text{MgH}_2$ phase. In all milled samples, with and without Ni, two desorption maxima are present. These maxima are a direct consequence of bimodal particle size distribution (Figs. 3 and 4). In the case of the addition of Ni, a catalytic effect is the most pronounced, especially in the sample $\text{MgH}_2 + 5 \text{ wt\% Ni}$ milled for 45 min due to excellent distribution of Ni in MgH_2 , confirmed by SED-EDS (Fig. 6 c).

In Fig. 9 the TPD profiles of as-received MgH_2 , milled MgH_2 , and $\text{MgH}_2 + 5 \text{ wt\% Ni}$ are shown. TPD analysis of as-received MgH_2 (Fig. 9, blue line) shows that hydrogen desorption begins at 441 °C while the desorption maximum is present at 480 °C. The presence of only one desorption maximum is following the literature data [10,43,44]. As shown in Fig. 9 (red line), hydrogen is released at lower temperatures in the case of the milled samples. The low-temperature (LT) maxima for the samples milled for 15 and 45 min are at 400 °C and 392 °C, while for the sample milled for 30 min, the maximum is at 366 °C. The high-temperature (HT) maximum for all the samples is at 440 °C, but the maximum narrows with the increase of milling time, i.e. hydrogen is released in a shorter time and temperature interval. In comparison with the results of TPD analysis and DSC analysis, we can conclude that the maximum at lower temperature belongs to the hydrogen desorbed from smaller particles, obtained after milling, while

Table 3 – Apparent activation energy (E_a) values obtained by Avrami – Erofeev model for $n = 3, 4$.

Sample	Peak	θ	E_a for $n = 4$ (kJ/mol)	E_a for $n = 3$ (kJ/mol)
As-received MgH_2	/	0.20–0.80	90 ± 2	124 ± 2
MgH_2 15min	LT	0.20–0.80	92 ± 2	126 ± 3
MgH_2 15min	HT	0.12–0.85	32.6 ± 0.4	47.6 ± 0.5
MgH_2 30min	LT	0.25–0.80	44.6 ± 0.4	63.4 ± 0.5
MgH_2 30min	HT	0.25–0.80	47.1 ± 0.6	66.8 ± 0.8
MgH_2 45min	LT	0.20–0.80	133 ± 3	181 ± 4
MgH_2 45min	HT	0.13–0.88	24.1 ± 0.2	36.0 ± 0.3
$MgH_2 + 5$ wt% Ni 15min	LT	0.15–0.85	26.6 ± 0.3	39.0 ± 0.4
$MgH_2 + 5$ wt% Ni 15min	HT	0.20–0.80	35.9 ± 0.4	51.9 ± 0.6
$MgH_2 + 5$ wt% Ni 30min	LT	0.10–0.60	45.1 ± 0.2	64.0 ± 0.2
$MgH_2 + 5$ wt% Ni 30min	HT	0.26–0.74	43.1 ± 0.5	61.3 ± 0.7
$MgH_2 + 5$ wt% Ni 45min	LT	0.20–0.70	27.7 ± 0.2	40.4 ± 0.3
$MgH_2 + 5$ wt% Ni 45min	HT	0.20–0.70	36.7 ± 0.4	52.3 ± 0.5

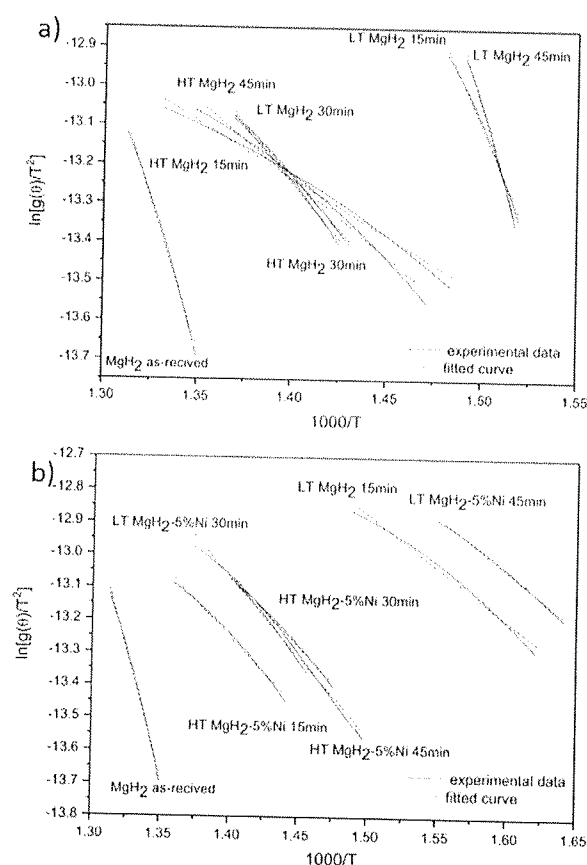


Fig. 10 – The plot of $\ln [g(\theta)/T^2]$ function vs. $1000/T$ for a) LT and HT maxima of MgH_2 . Experimental data and fit with the best linearity obtained for nucleation model $g(\theta) = [-\ln(1-\theta)]^{(1/n)}$, for $n = 3$ b) LT and HT maxima of $MgH_2 + 5$ wt% Ni. Experimental data and fit with the best linearity obtained for nucleation model $g(\theta) = [-\ln(1-\theta)]^{(1/n)}$, for $n = 4$.

the more intense maximum is at higher temperature and it originate from presence of hydrogen desorbed from $\beta - MgH_2$ and agglomerates [43].

Desorption temperatures for milled $MgH_2 + 5$ wt% Ni (black line) are slightly lower regarding to the desorption temperatures for the milled pure MgH_2 , and as much as $110-40$ °C lower than the hydrogen desorption temperature for the as-received MgH_2 . The first maximum for all samples is evident at 370 °C, approximately. The maxima of the samples milled for 15, 30, and 45 min are at 429 °C, 423 °C, and 441 °C. The second maximum becomes narrower with the increase of milling time, i.e. the hydrogen is released over a shorter period of time in a linear temperature range which is a consequence of the catalytic effect of nickel.

Kinetic models for the hydrogen desorption process were investigated. The activation energy values are obtained (Table 3) by fitting experimental data to the kinetics models. The samples, in which unequivocal observation of the desorption maximum was possible, were examined: as-received MgH_2 , MgH_2 milled for 30 min and $MgH_2 + 5$ wt% Ni milled for 30 and 45 min. The kinetic model Avrami-Erofeev showed the best linearity (Fig. 10) with $n = 3$ and $n = 4$ which is described by a function:

$$g(\theta) = [-\ln(1-\theta)]^{1/n}$$

where n is reaction order and represents the sum of λ and β . λ is the dimensionality factor and it describes the dimensional growth of nucleation nuclei. It has values 3, 2 and 1. When $\lambda = 1$, we have one-dimensional (1D) growth of the nucleus of the formed phase, $\lambda = 2$ - 2D growth, and when $\lambda = 3$ there is three-dimensional (3D) growth of magnesium nucleation nuclei. Factor β is constant and describes the character of the process. It adopt values of 0 and 1 depending on whether the number of growing nuclei is constant or it changes [44]. It is assumed that hydrogen desorption reaction is a 4th order reaction. The growth of magnesium nuclei considers to be three-dimensional (3D). It is observed extensive difference in values of apparent activation energy for low-temperature (LT) and high-temperature (HT) maxima for MgH_2 milled for 30 and 45 min is observed (Table 3, Fig. 10).

The value of apparent activation energy (E_a) of MgH_2 milled for 30 min is twice as less than the value of the as-received MgH_2 , which can be explained with by the reduction of the particle size. In $MgH_2 + 5$ wt% Ni sample with the same milling

time, it has been noticed that values of E_a are lower by several kJ/mol due to the catalytic effect of Ni. The sample with the addition of nickel milled for 45 min has the lowest value of $E_a = 27.7$ kJ/mol for the LT maximum, and 36.7 kJ/mol for the HT maximum. Those values are in correlation with the assumption that with the longer milling time the dispersion of nickel is better in MgH_2 bulk, which has catalytic effect on the hydrogen desorption reaction [16,22,23]. The catalytic effect of Ni on H_2 desorption from MgH_2 by lowering E_a was proved by Hanada et al. [21] who found that by incorporating the 2 mol% of Ni and grinding for 15 min, the activation energy for the dehydrogenation reaction was 94 kJ/mol. Similarly, Xie et al. [39] discovered that by adding 10 wt% Ni and grinding for 2 h, the activation energy is 118 kJ/mol while the addition of 25 wt % Ni, reduced the activation energy to 82 kJ/mol. On the other hand, Cova et al. [45] were able to decrease the activation energy to 117 kJ/mol by grinding MgH_2 with 1 mol% Ni for 10 h. Yang et al. have obtained a similar value of E_a 83 kJ/min for the sample with the addition of 5 wt% Ni milled for 3 h [42]. The decrease in value of E_a is a direct consequence of the uniform dispersion of nickel particles in MgH_2 (Fig. 6 SEM-EDS) with the increase of milling time. The catalytic effect of Ni can be explained through effects of physical interface between metal catalyst and investigated metal-hydride (MgH_2). Ouyang et al. [46] assert that reduction of desorption temperature is a direct consequence of change of interface energy along high interface density. In sample $MgH_2 + 5$ wt% Ni milled for 45 min, Ni is highly distributed in the MgH_2 matrix, reaching high interface density. In the interface, extra energy is stored, and it can reduce the energy barrier for formation of new phases. Metal catalysts with good, homogeneous dispersion in matrix, provide more reaction sites and diffusion channels and desorption occurs over edge sites [24,25]. After dehydrogenation of the sample, formation of new phase Mg_2Ni was proved [24–26] which have a key role in accelerating of further sorption reaction. Finally, Mg_2Ni phase would act as a “hydrogen pump” in further absorption/desorption cycles [32,33] by destabilizing Mg–H bond of MgH_2 and facilitate hydrogen dissociation due to high affinity toward hydrogen [31,34].

Conclusions

Two main processes, grinding and catalytic effect, are separately analyzed in MgH_2 –Ni solid-state system. By applying short milling intervals, MgH_2 –Ni system has shown adequate behavior as a medium for hydrogen storage. The SEM-EDS measurements confirmed uniform distribution of Ni particles in MgH_2 powder for milling interval of 45 min, but morphological and microstructural properties of MgH_2 –Ni system are not significantly changed. As a consequence of better Ni particle distribution, in comparison with pure MgH_2 , lower apparent activation energy (E_a) and H_2 desorption temperature are noticed. The best explanation of hydrogen desorption reaction shows Avrami-Erofeev model, for parameter $n = 4$. Based on SEM, TPD, and kinetic model fitting, two very important consequences are obvious: the influence of mechanochemical grinding of materials is minimized, while the dependence of the nickel powder distribution in MgH_2 bulk on the milling time is dominant. By using short

milling times, grinding effect was minimized and the only predominant effect is the catalytic effect of Ni on the H_2 desorption from MgH_2 .

Declaration of competing interest

The authors declare that they have no known competing financial interests or personal relationships that could have appeared to influence the work reported in this paper.

Acknowledgements

This paper is supported by the Ministry of Science, Technological Development and Innovation of the Republic of Serbia, under Grants No. 451-03-47/2023-01/200017 and No. 451-03-47/2023-01/200175.

REFERENCES

- [1] Schlapbach L, Züttel A. Hydrogen-storage materials for mobile applications. *Nature* 2001;414:353–8. <https://doi.org/10.1038/35104634>.
- [2] Züttel A, Remhof A, Borgschulte A, Friedrichs O. Hydrogen: the future energy carrier. *Philos Trans R Soc A Math Phys Eng Sci* 2010;368:3329–42. <https://doi.org/10.1098/rsta.2010.0113>.
- [3] Koroneos C, Dompros A, Roumbas G, Moussiopoulos N. Advantages of the use of hydrogen fuel as compared to kerosene. *Resour Conserv Recycl* 2005;44:99–113. <https://doi.org/10.1016/j.resconrec.2004.09.004>.
- [4] Sakintuna B, Lamari-Darkrim F, Hirscher M. Metal hydride materials for solid hydrogen storage: a review. *Int J Hydrogen Energy* 2007;32:1121–40. <https://doi.org/10.1016/j.ijhydene.2006.11.022>.
- [5] Huang ZG, Guo ZP, Calka A, Wexler D, Wu J, Notten PHL, et al. Noticeable improvement in the desorption temperature from graphite in rehydrogenated MgH_2 /graphite composite. *Mater Sci Eng, A* 2007;447:180–5. <https://doi.org/10.1016/j.msea.2006.11.074>.
- [6] Markman E, Luzzatto-Shukrun L, Levy YS, Pri-Bar I, Gelbstein Y. Effect of additives on hydrogen release reactivity of magnesium hydride composites. *Int J Hydrogen Energy* 2022;47:31381–94. <https://doi.org/10.1016/j.ijhydene.2022.07.025>.
- [7] Kurko S, Milanović I, Milošević S, Rašković-Lovre Ž, Fernández JF, Ares Fernandez JR, et al. Changes in kinetic parameters of decomposition of MgH_2 destabilized by irradiation with C^{2+} ions. *Int J Hydrogen Energy* 2013;38:12199–206. <https://doi.org/10.1016/j.ijhydene.2013.05.132>.
- [8] Kurko S, Milanović I, Grbović Novaković J, Ivanović N, Novaković N. Investigation of surface and near-surface effects on hydrogen desorption kinetics of MgH_2 . *Int J Hydrogen Energy* 2014;39:862–7. <https://doi.org/10.1016/j.ijhydene.2013.10.107>.
- [9] Matović L, Kurko S, Rašković-Lovre Ž, Vujasin R, Milanović I, Milošević S, et al. Assessment of changes in desorption mechanism of MgH_2 after ion bombardment induced destabilization. *Int J Hydrogen Energy* 2012;37:6727–32. <https://doi.org/10.1016/j.ijhydene.2012.01.084>.
- [10] Pantić T, Milanović I, Lukić M, Grbović Novaković J, Kurko S, Biliškov N, et al. The influence of mechanical milling

- parameters on hydrogen desorption from MgH₂-W₂O₃ composites. *Int J Hydrogen Energy* 2020;45:7901–11. <https://doi.org/10.1016/j.ijhydene.2019.07.167>.
- [11] Ma LP, Wang P, Cheng HM. Hydrogen sorption kinetics of MgH₂ catalyzed with titanium compounds. *Int J Hydrogen Energy* 2010;35:3046–50. <https://doi.org/10.1016/j.ijhydene.2009.07.014>.
 - [12] Barkhordarian G, Klassen T, Bormann R. Fast hydrogen sorption kinetics of nanocrystalline Mg using Nb₂O₅ as catalyst. *Scripta Mater* 2003;49:213–7. [https://doi.org/10.1016/S1359-6462\(03\)00259-8](https://doi.org/10.1016/S1359-6462(03)00259-8).
 - [13] Oelerich W, Klassen T, Bormann R. Metal oxides as catalysts for improved hydrogen sorption in nanocrystalline Mg-based materials. *J Alloys Compd* 2001;315:237–42. [https://doi.org/10.1016/S0925-8388\(00\)01284-6](https://doi.org/10.1016/S0925-8388(00)01284-6).
 - [14] Zaluska A, Zaluski L, Ström-Olsen JO. Nanocrystalline magnesium for hydrogen storage. *J Alloys Compd* 1999;288:217–25. [https://doi.org/10.1016/S0925-8388\(99\)00073-0](https://doi.org/10.1016/S0925-8388(99)00073-0).
 - [15] Jung KS, Lee EY, Lee KS. Catalytic effects of metal oxide on hydrogen absorption of magnesium metal hydride. *J Alloys Compd* 2006;421:179–84. <https://doi.org/10.1016/j.jallcom.2005.09.085>.
 - [16] Liang G, Huot J, Boily S, Van Neste A, Schulz R. Hydrogen storage properties of the mechanically milled MgH₂-V nanocomposite. *J Alloys Compd* 1999;291:295–9. [https://doi.org/10.1016/S0925-8388\(99\)00268-6](https://doi.org/10.1016/S0925-8388(99)00268-6).
 - [17] Gennari FC, Castro FJ, Urretavizcaya G, Meyer G. Catalytic effect of Ge on hydrogen desorption from MgH₂. *J Alloys Compd* 2002;334:277–84. [https://doi.org/10.1016/S0925-8388\(01\)01786-8](https://doi.org/10.1016/S0925-8388(01)01786-8).
 - [18] Blanchard D, Brinks HW, Hauback BC, Norby P. Desorption of LiAlH₄ with Ti- and V-based additives. *Mater Sci Eng B Solid-State Mater Adv Technol* 2004;108:54–9. <https://doi.org/10.1016/j.mseb.2003.10.114>.
 - [19] Aguey-Zinsou KF, Ares Fernandez JR, Klassen T, Bormann R. Effect of Nb₂O₅ on MgH₂ properties during mechanical milling. *Int J Hydrogen Energy* 2007;32:2400–7. <https://doi.org/10.1016/j.ijhydene.2006.10.068>.
 - [20] Andreasen A. Effect of Ti-doping on the dehydrogenation kinetic parameters of lithium aluminum hydride. *J Alloys Compd* 2006;419:40–4. <https://doi.org/10.1016/j.jallcom.2005.09.067>.
 - [21] Hanada N, Ichikawa T, Fujii H. Catalytic effect of nanoparticle 3d-transition metals on hydrogen storage properties in magnesium hydride MgH₂ prepared by mechanical milling. *J Phys Chem B* 2005;109:7188–94. <https://doi.org/10.1021/jp044576c>.
 - [22] Xie, Shuai L, J Shan Li, Zhang T Bang, Chao Kou H. Role of milling time and Ni content on dehydrogenation behavior of MgH₂/Ni composite. *Trans Nonferrous Met Soc China* 2017;27:569–77. [https://doi.org/10.1016/S1003-6326\(17\)60063-3](https://doi.org/10.1016/S1003-6326(17)60063-3).
 - [23] Shimada M, Higuchi E, Inoue H. Hydrogen desorption properties of MgH₂-Ni-Ni₂Si Composites prepared by mechanochemical method. *J Alloys Compd* 2013;580:0–11. <https://doi.org/10.1016/j.jallcom.2013.01.191>.
 - [24] Gao D, Zhang L, Song M, Wu F, Wang J, Zhao H, et al. Interfacial engineering of nickel/vanadium based two-dimensional layered double hydroxide for solid-state hydrogen storage in MgH₂. *Int J Hydrogen Energy* 2022;48:9390–400. <https://doi.org/10.1016/j.ijhydene.2022.12.032>.
 - [25] Hu C, Zheng Z, Si T, Zhang Q. Enhanced hydrogen desorption kinetics and cycle durability of amorphous TiMgVNi₃-doped MgH₂. *Int J Hydrogen Energy* 2022;47:3918–26. <https://doi.org/10.1016/j.ijhydene.2021.11.010>.
 - [26] Tan D, Peng C, Zhang Q. ScienceDirect Microstructural characteristics and hydrogen storage properties of the Mg e Ni e TiS₂ nanocomposite prepared by a solution-based method. *Int J Hydrogen Energy* 2023;1–13. <https://doi.org/10.1016/j.ijhydene.2023.01.185>.
 - [27] Jangid MK, Sharma SS, Ray J, Yadav DK, Lal C. Structural, optical and electrical characterizations of Mg/Ti/Ni multilayer thin films deposited by DC magnetron sputtering for hydrogen storage. *Int J Hydrogen Energy* 2023. <https://doi.org/10.1016/j.ijhydene.2022.11.324>.
 - [28] Liang G, Huot J, Boily S, Van Neste A, Schulz R. Catalytic effect of transition metals on hydrogen sorption in nanocrystalline ball milled MgH₂-Tm (Tm = Ti, V, Mn, Fe and Ni) systems. *J Alloys Compd* 1999;292:247–52. [https://doi.org/10.1016/S0925-8388\(99\)00442-9](https://doi.org/10.1016/S0925-8388(99)00442-9).
 - [29] Huot J, Akiba E, Takada T. Mechanical alloying of MgNi compounds under hydrogen and inert atmosphere. *J Alloys Compd* 1995;231:815–9. [https://doi.org/10.1016/0925-8388\(95\)01764-X](https://doi.org/10.1016/0925-8388(95)01764-X).
 - [30] El-Eskandarany MS, Shaban E, Ali N, Aldakheel F, Alkandary A. In-situ catalyzation approach for enhancing the hydrogenation/dehydrogenation kinetics of MgH₂ powders with Ni particles. *Sci Rep* 2016;6:1–13. <https://doi.org/10.1038/srep37335>.
 - [31] Peng C, Li Y, Zhang Q. Enhanced hydrogen desorption properties of MgH₂ by highly dispersed Ni: the role of in-situ hydrogenolysis of nickelocene in ball milling process. *J Alloys Compd* 2022;900:163547. <https://doi.org/10.1016/j.jallcom.2021.163547>.
 - [32] Ding Z, Li Y, Yang H, Lu Y, Tan J, Li J, et al. Tailoring MgH₂ for hydrogen storage through nanoengineering and catalysis. *J Magnesium Alloys* 2022;10:2946–67. <https://doi.org/10.1016/j.jma.2022.09.028>.
 - [33] Huang T, Huang X, Hu C, Wang J, Liu H, Ma Z, et al. Enhancing hydrogen storage properties of MgH₂ through addition of Ni/CoMoO₄ nanorods. *Mater Today Energy* 2021;19:100613. <https://doi.org/10.1016/j.mtener.2020.100613>.
 - [34] Zhang QA, Liu DD, Wang QQ, Fang F, Sun DL, Ouyang LZ, et al. Superior hydrogen storage kinetics of Mg₁₂YNi alloy with a long-period stacking ordered phase. *Scripta Mater* 2011;65:233–6. <https://doi.org/10.1016/j.scriptamat.2011.04.014>.
 - [35] Andreasen A, Vegge T, Pedersen AS. Compensation effect in the hydrogenation/dehydrogenation kinetics of metal hydrides. *J Phys Chem B* 2005;109:3340–4. <https://doi.org/10.1021/jp0458755>.
 - [36] Gasan H, Celik ON, Aydinbeyli N, Yaman YM. Effect of V, Nb, Ti and graphite additions on the hydrogen desorption temperature of magnesium hydride. *Int J Hydrogen Energy* 2012;37:1912–8. <https://doi.org/10.1016/j.ijhydene.2011.05.086>.
 - [37] Dehouche Z, Djaozandry R, Huot J, Boily S, Goyette J, Bose TK, et al. Influence of cycling on the thermodynamic and structure properties of nanocrystalline magnesium based hydride. *J Alloys Compd* 2000;305:264–71. [https://doi.org/10.1016/S0925-8388\(00\)00718-0](https://doi.org/10.1016/S0925-8388(00)00718-0).
 - [38] Bassetti A, Bonetti E, Pasquini L, Montone A, Grbovic J, Antisari MV. Hydrogen desorption from ball milled MgH₂ catalyzed with Fe. *Eur Phys J B* 2005;43:19–27. <https://doi.org/10.1140/epjb/e2005-00023-9>.
 - [39] Xie L, Liu Y, Zhang X, Qu J, Wang Y, Li X. Catalytic effect of Ni nanoparticles on the desorption kinetics of MgH₂ nanoparticles. *J Alloys Compd* 2009;482:388–92. <https://doi.org/10.1016/j.jallcom.2009.04.028>.
 - [40] Xi S, Wang X, Torne KC, Zhang T, Han Z, Gao M, et al. Effect of Ni and SAPO-34 co-additive on enhancing hydrogen storage performance of MgH₂. *Int J Hydrogen Energy*

- 2021;46:23748–56. <https://doi.org/10.1016/j.ijhydene.2021.04.177>.
- [41] Varin RA, Czujko T, Wasmund EB, Wronski ZS. Hydrogen desorption properties of MgH₂ nanocomposites with nano-oxides and Inco micrometric- and nanometric-Ni. *J Alloys Compd* 2007;446–447:63–6. <https://doi.org/10.1016/j.jallcom.2006.10.134>.
- [42] Yang X, Hou Q, Yu L, Zhang J. Improvement of the hydrogen storage characteristics of MgH₂ with a flake Ni nano-catalyst composite. *Dalton Trans* 2021;50:1797–807. <https://doi.org/10.1039/d0dt03627g>.
- [43] Varin RA, Czujko T, Wronski Z. Particle size, grain size and γ -MgH₂ effects on the desorption properties of nanocrystalline commercial magnesium hydride processed by controlled mechanical milling. *Nanotechnology* 2006;17:3856–65. <https://doi.org/10.1088/0957-4484/17/15/041>.
- [44] Milanović I, Milošević S, Matović L, Vujasin R, Novaković N, Checchetto R, et al. Hydrogen desorption properties of MgH₂/LiAlH₄ composites. *Int J Hydrogen Energy* 2013;38:12152–8. <https://doi.org/10.1016/j.ijhydene.2013.05.020>.
- [45] Cova F, Arneodo Larochette P, Gennari F. Hydrogen sorption in MgH₂-based composites: the role of Ni and LiBH₄ additives. *Int J Hydrogen Energy* 2012;37:15210–9. <https://doi.org/10.1016/j.ijhydene.2012.07.132>.
- [46] Ouyang LZ, Ye SY, Dong HW, Zhu M. Effect of interfacial free energy on hydriding reaction of Mg-Ni thin films. *Appl Phys Lett* 2007;90:2–5. <https://doi.org/10.1063/1.2428877>.

Article

The Catalytic Effect of Vanadium on Sorption Properties of MgH₂-Based Nanocomposites Obtained Using Low Milling Time

Zorana Sekulić ¹, Jasmina Grbović Novaković ^{2,*}, Bojana Babić ², Milica Prvulović ², Igor Milanović ², Nikola Novaković ², Dragan Rajnović ³, Nenad Filipović ⁴ and Vanja Asanović ⁵

- ¹ Directorate for Energy and Energy Efficiency, Ministry of Capital Investments, The Government of Montenegro, Rimski trg 46, 81000 Podgorica, Montenegro
 - ² Centre of Excellence for Renewable and Hydrogen Energy, Vinča Institute of Nuclear Sciences, National Institute of Republic of Serbia, University of Belgrade, Mike Petrovića Alasa 12-14, 11000 Belgrade, Serbia; bojana.babic@vin.bg.ac.rs (B.B.); igorm@vin.bg.ac.rs (I.M.)
 - ³ Faculty of Technical Sciences, University of Novi Sad, Trg Dositeja Obradovića 6, 21000 Novi Sad, Serbia
 - ⁴ Institute of Technical Sciences of Serbian Academy of Science and Arts, Knez Mihajlova 35, 11000 Belgrade, Serbia
 - ⁵ Faculty of Metallurgy and Technology, University of Montenegro, Cetinjski Put 2, 81000 Podgorica, Montenegro
- * Correspondence: jasnag@vin.bg.ac.rs

Abstract: The effects of catalysis using vanadium as an additive (2 and 5 wt.%) in a high-energy ball mill on composite desorption properties were examined. The influence of microstructure on the dehydration temperature and hydrogen desorption kinetics was monitored. Morphological and microstructural studies of the synthesized sample were performed by X-ray diffraction (XRD), laser particle size distribution (PSD), and scanning electron microscopy (SEM) methods, while differential scanning calorimetry (DSC) determined thermal properties. To further access amorph species in the milling blend, the absorption spectra were obtained by FTIR-ATR analysis (Fourier transform infrared spectroscopy attenuated total reflection). The results show lower apparent activation energy (E_{app}) and H₂ desorption temperature are obtained for milling blend with 5 wt.% added vanadium. The best explanation of hydrogen desorption reaction shows the Avrami-Erofeev model for parameter $n = 4$. Since the obtained value of apparent activation energy is close to the Mg-H bond-breaking energy, one can conclude that breaking this bond would be the rate-limiting step of the process.

Keywords: hydrogen storage; magnesium hydride; transition metals; additives; mechanochemistry

check for updates

Citation: Sekulić, Z.; Novaković, J.G.; Babić, B.; Prvulović, M.; Milanović, I.; Novaković, N.; Rajnović, D.; Filipović, N.; Asanović, V. The Catalytic Effect of Vanadium on Sorption Properties of MgH₂-Based Nanocomposites Obtained Using Low Milling Time. *Materials* **2023**, *16*, 5480. <https://doi.org/10.3390/ma16155480>

Academic Editor: Karol J. Fijałkowski

Received: 13 April 2023

Revised: 3 June 2023

Accepted: 7 June 2023

Published: 5 August 2023



Copyright: © 2023 by the authors. Licensee MDPI, Basel, Switzerland. This article is an open access article distributed under the terms and conditions of the Creative Commons Attribution (CC BY) license (<https://creativecommons.org/licenses/by/4.0/>).

1. Introduction

Hydrogen as an energy vector represents great potential due to its high gravimetric density and low mass, as well as the fact that combustion does not emit harmful chemical byproducts. Hydrogen has the highest energy density per unit mass compared to any other fuel but a rather low energy density per unit volume. Further, hydrogen storage is a key technology for developing a hydrogen and fuel cell-based economy [1]. Metal hydrides as alternative hydrogen carriers have various performance parameters such as operating temperature, sorption kinetics, activation conditions, cyclic options, and equilibrium hydrogen pressure. These parameters can be improved or adjusted to meet the technical requirements of different applications [2]. Hydrogen in metal hydrides is chemically bonded, usually much stronger than the physical bonding present during hydrogen adsorption. Consequently, more energy is needed to release chemically bound hydrogen [3]. On the other hand, a stronger bond between hydrogen and metal hydride allows the storage of higher hydrogen densities even under ambient conditions [4]. Magnesium hydride is recognized as an excellent material for solid-state hydrogen storage due to its high

gravimetric hydrogen capacity, good reversibility, and low cost. However, its practical application is limited by high thermodynamic stability and slow sorption kinetics [5]. To overcome the mentioned shortcomings, most of the research on magnesium hydride-based materials focuses on improving volumetric and gravimetric capacities, hydrogen absorption/desorption kinetics, and thermodynamics [1–5]. Mechanochemical modifications of the crystal structure of magnesium hydride and doping with the transition metals is a possible path for improving sorption properties. Doping with transition metals and their alloys is generally considered the simplest method to accelerate the sorption kinetics of MgH_2 . Most of the activities done in this field to the present day have been devoted to mechanochemical modifications using long milling times [1–16]. Sun et al. [4] compared the influence of transition metals in combination with carbon materials on the storage properties of hydrogen in MgH_2 . The desorption properties of the tested systems can be ranked as follows: $\text{Mg-Ti} > \text{Mg-Nb} > \text{Mg-Ni} > \text{Mg-V} > \text{Mg-Co} > \text{Mg-Mo}$. These composites can release hydrogen at temperatures below 225 °C, significantly lower than pure MgH_2 . Liang et al. [6] investigated the influence of 3d transition metals Ti, V, Mn, Fe, and Ni as additives on the sorption properties of MgH_2 , where powder nanocomposites were synthesized by a 20 h milling process. Desorption was fastest in the system $\text{MgH}_2\text{-V}$, then $\text{MgH}_2\text{-Ti}$, $\text{MgH}_2\text{-Fe}$, $\text{MgH}_2\text{-Ni}$, and $\text{MgH}_2\text{-Mn}$ at lower temperatures. On the other hand, the fastest absorption kinetics were determined for Mg-Ti , then Mg-V , Mg-Fe , Mg-Mn , and finally Mg-Ni . Of the investigated transition metals, V and Ti showed a better catalytic effect than Ni during hydrogen absorption and desorption. Composites with V or Ti as an additive showed fast desorption kinetics above 250 °C and absorption kinetics at temperatures below 30 °C. When examining the desorption properties of an $\text{MgH}_2\text{-V}$ system prepared by ball milling, Liang et al. [7] concluded that MgH_2 – 5 at.% V can desorb hydrogen at 200 °C and reabsorb hydrogen faster even at room temperature. It was found that the apparent activation energy of hydrogen desorption was reduced to 62 kJ/mol. Gasan et al. [8] investigated the influence of 5 wt.% of additives (V, Nb, and Ti) on the desorption temperature of hydrogen in MgH_2 . X-ray powder diffraction (XRD) results showed that adding vanadium powder significantly affected the transformation of Mg to MgO or hydride because the amount of MgO in the $\text{MgH}_2\text{-V}$ system was higher than in other systems. Scanning electron microscopy also showed a significant reduction in the particle size of the powder. The results obtained by differential scanning calorimetry showed that the addition of 5 wt.% additive reduces the desorption temperature of hydrogen in MgH_2 by about 40–50 °C. Lu et al. [9] investigated the catalytic effect of two-dimensional (2D) vanadium nanoplates (VNS) on MgH_2 for hydrogen storage purposes. It was found that the composite MgH_2 + 7 wt.% VNS begins to release hydrogen at 187.2 °C, or at a temperature 152 °C lower than MgH_2 without additives. Within 10 min at 300 °C, 6.3 wt.% of hydrogen was released from MgH_2 + 7 wt.% of VNS composites. Additionally, a completely dehydrated sample can absorb hydrogen at room temperature under a hydrogen pressure of 3.2 MPa. Hanada et al. [10] investigated the catalytic effect of nanoparticles on 3d transition metals on hydrogen desorption in MgH_2 prepared by ball milling. All MgH_2 composites prepared by adding a small amount of Fe, Co, Ni, and Cu metal nanoparticles and ball milling for 2 h show much better hydrogen desorption than pure MgH_2 . The best properties were observed for an MgH_2 -based composite doped with 2 mol.% Ni nanoparticles and prepared by short-term (15 min) low-intensity ball milling (200 rpm). A large amount of hydrogen (~6.5 wt.%) was found to be desorbed in the temperature range from 150 °C to 250 °C by heating at a rate of 5 °C/min under a flow of He gas, practically without partial hydrogen pressure. According to DFT calculations done by Paskaš Mamula et al. [11], adding Fe, Ni, and Co will improve desorption kinetics due to the higher stability of Tm-H bonds. The final remark of numerous scientific papers on this topic is that transition metals have great potential in the choice of dopants from the aspect of improving sorption kinetics and reducing the activation energy of hydrogen desorption. On the other hand, most of the studies presented so far used similar high-energy mills and concerned milling at long times, from 1 to 25 h [1–10,12–17]. Further, as observed by Czujko et al. [18] there is not

much difference in sorption kinetics of the mechanically modified MgH_2 due to changes in the particle and crystallite size of the powder particles. Therefore, it is difficult to determine a parameter that influences kinetics.

In this paper, we have examined the structural transformations that occur in doped MgH_2 systems with different concentrations of vanadium at low milling times ranging from 15 to 45 min and correlated to the thermal behavior of the samples and kinetics.

2. Materials and Methods

Magnesium hydride (Langfang GreatAP Chemicals Co., Langfang, China, purity 98%) with the addition of vanadium (Merck, Rahway, NJ, USA, purity 99.99%) in different weight percentages (2 and 5 wt.%) was synthesized at different time intervals (15, 30, and 45 min) in an inert argon atmosphere to prevent oxidation of the sample, using BPR (Ball to Powder Ratio) $\approx 10:1$. Mechanochemical synthesis was done in the SPEX Sample Mixer/Mill 5100 mill using stainless steel vial and balls, stainless steel jars, vials 1.2", 1 gr balls, with a total of 100 mg sample amount [19]. The intensity of ball milling was 2500 rpm. The composition and parameters of milling are given in Table 1.

Table 1. The list of prepared samples and milling conditions.

Composition	wt.% V	Milling Time [min]	Name
$\text{MgH}_2 + \text{V}$	2	15	2V15
		30	2V30
		45	2V45
	5	15	5V15
		30	5V30
		34	5V45

Structural characterization of material was performed using X-ray diffraction analysis (XRD) on a Rigaku Ultima IV diffractometer using a nickel filter and $\text{Cu K}\alpha$ radiation (while wavelength was 0.1540 nm), in the 2θ range between 20 and 90° , at operating parameters of 40 kV and 40 mA, a step of 0.02° , the accumulative time of 5 s in every point and a silicon strip detector counter. The particle size distribution was analyzed using Mastersizer 2000, (Malvern Instruments Ltd., Malvern, UK) according to the standard procedure explained by Milanović et al. [20]. The desorption properties of the milled samples were measured by DSC apparatus SETARAM DSC131 using a heating rate of $10^\circ\text{C}/\text{min}$, and temperature-programmed desorption (TPD) using homemade apparatus equipped with a mass spectrometer Extorr 300 at the same heating rate [21]. Iso-conventional kinetic methods and the Avrami-Erofeev kinetic model are described elsewhere [21].

3. Results

3.1. Microstructural and Morphological Characterization

As shown in Figure 1, sharp diffraction maxima at positions $2\theta = 27.63^\circ$ (110), 35.62° (101), 39.48° (200), 54.21° (211), are characteristic of $\beta\text{-MgH}_2$ with tetragonal structure, space group P_{42}/mm (No. 136) [22]. Low-intensity diffraction maxima at $2\theta = 32.18^\circ$ (100) and 36.63° (101) originating from metallic Mg as expected given the initial composition of the sample (98% purity). There are no peaks corresponding to the crystalline phases of $\text{Mg}(\text{OH})_2$ and MgO .

Figure 2 shows diffractograms of all samples obtained using different milling times. The tetragonal $\beta\text{-MgH}_2$ is the dominant phase, although a small amount of $\gamma\text{-MgH}_2$ phase is present in samples even after 15 min of milling. The intensity of $\gamma\text{-MgH}_2$ diffraction maxima increases with the increase of milling time since the amount of $\gamma\text{-MgH}_2$ increases. The broadening of $\beta\text{-MgH}_2$ phase diffraction maxima is visible, too, indicating a decrease in crystallite size. A similar was found by Varin et al. [23]. They have shown a spread of diffraction maxima in $\beta\text{-MgH}_2$ that increases with increasing milling time. The authors

associated this phenomenon with a decrease in crystallite size, which may be accompanied by the appearance of lattice micro-stress. Mixing with additives also introduces stress into the lattice, leading to peak broadening [12]. We expect similar behavior of samples milled with vanadium (see Table 2).

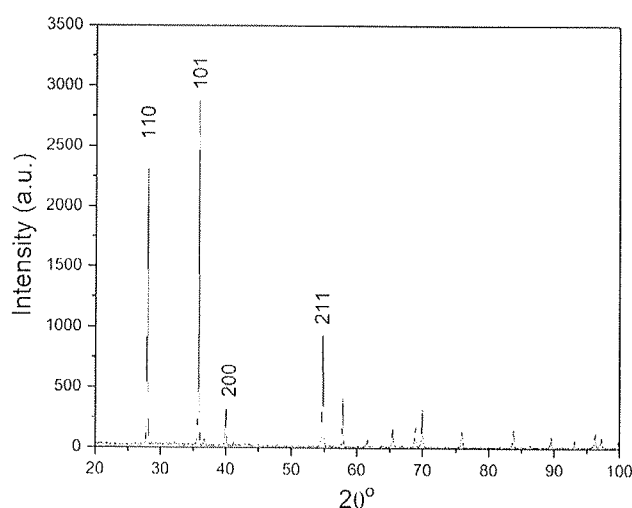


Figure 1. XRD pattern of as-received MgH_2 .

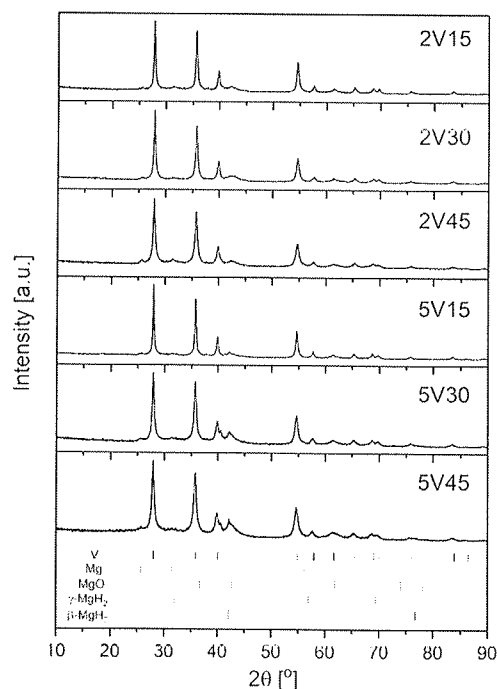


Figure 2. Diffractograms of milled MgH_2 -V composites obtained with different quantities of Vanadium (2 and 5 wt.%) and milled for 15–45 min.

Table 2. Crystallite size dependence on milling time and chemical composition.

V Content (wt.%)/Milling Time (s)	15	30	45
0	20	39	30
2	39	35	30
5	46	30	25

FTIR-ATR spectra for the samples milled with 2 and 5 wt.% of vanadium, are given in Figure 3a,b, respectively. Three regions are clearly distinguished: the first ($500\text{--}800\text{ cm}^{-1}$) corresponds to Mg-H bending vibrations, the second ($900\text{--}1300\text{ cm}^{-1}$) corresponds to Mg-H stretching vibrations [24], and for the 2V15 sample, and the third region ($2500\text{--}3900\text{ cm}^{-1}$) corresponds to the observed OH group vibrations. For all three 5V samples, OH vibrations at 3670 cm^{-1} are observed. The largest changes are observed in the region 900 cm^{-1} FTIR-ATR spectra of MgH_2 samples milled with 2 wt.% V (a) and 5 wt.% V (b) samples.

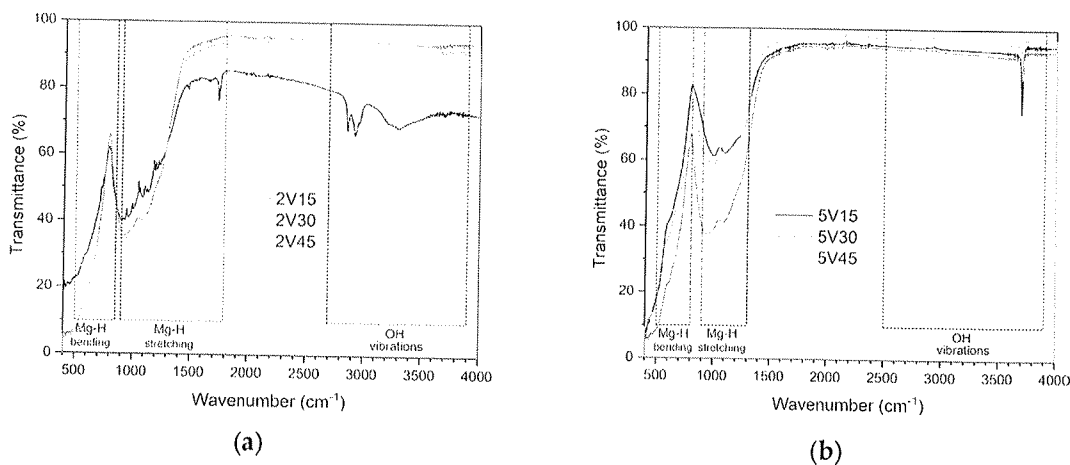


Figure 3. FTIR-ATR spectra of samples of MgH_2 samples milled with 2 wt.% V (a) and 5 wt.% V (b) samples.

Figure 4 shows the comparative distribution of particle sizes for all samples. As shown in Figure 4a, for all three milled blends with 2 wt.% of vanadium, about 30% of the particles have an average particle size of about $1\text{ }\mu\text{m}$. Sample 2V15 has about 70% of particles with an average size of about $10\text{ }\mu\text{m}$. As milling time increases, the average particle sizes increase due to agglomeration, and distribution becomes polymodal. This is followed by the specific surface area decrease of almost 50% for 2V and 5V samples. In Figure 4b the particle size distribution of samples milled with 5 wt.% of vanadium for different milling times: 15, 30, and 45 min (5V15, 5V30, and 5V45). The 5V15 sample has a particle size distribution in the range of $0.2\text{--}91.2\text{ }\mu\text{m}$ (about 75% of the sample is in the range of $0.2\text{--}10\text{ }\mu\text{m}$, with an average value of $2.5\text{ }\mu\text{m}$, while about 25% of the sample is in the range of $10\text{--}91.2\text{ }\mu\text{m}$, with the medium particle size of $39.3\text{ }\mu\text{m}$).

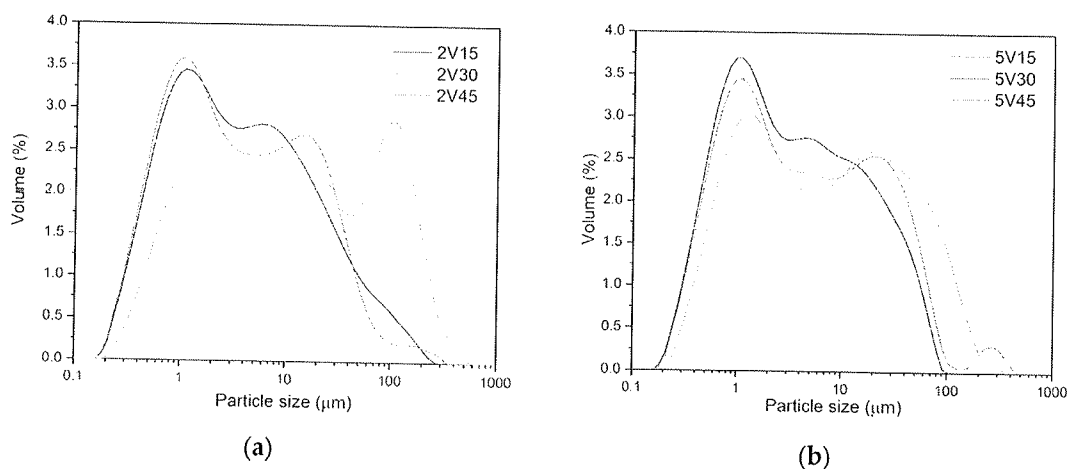


Figure 4. Particle size distribution of MgH_2 samples milled with 2 wt.% V (a) and 5 wt.% V (b) samples.

The 5V30 sample is characterized by the widest distribution of particle sizes, polymodally distributed, where 65% of the sample consists of particles of 0.2–10 μm , with an average particle size of 2.3 μm . In the range of 10–100 μm , there is 30% of the sample, with an average particle size of 39.3 μm . The residue is outside this range, i.e., 100–416 μm , with an average particle size of 229 μm . The 5V45 sample has a similar polymodal particle size distribution as the 5V30 sample. Here, in the range of 0.2–10 μm , almost 60% of the sample is present, with an average particle size of about 2.62 μm ; in the range of 10–100 μm there is about 37% of the sample, with an average particle size of 39.3 μm and the rest of the 5V45 sample powder consists of particles above 100 μm (from 100–316 μm) with an average particle size of 140 μm . Mechanical milling by adding 5 wt.% of the catalyst changes the shape of the distribution. However, as with the milled commercial material, the distribution is bimodal, except for the 5V30 sample, where the distribution is polymodal.

The images obtained by SEM analysis (Figure 5) correlate with the particle size distribution analysis results. Commercial powder particles are irregular in shape with a layered structure, rough on the surface with a size above 100 μm , while powder particles MgH_2 mechanically milled for 10 h are spongy in structure, with different sizes ranging from below 1 μm to 50 μm .

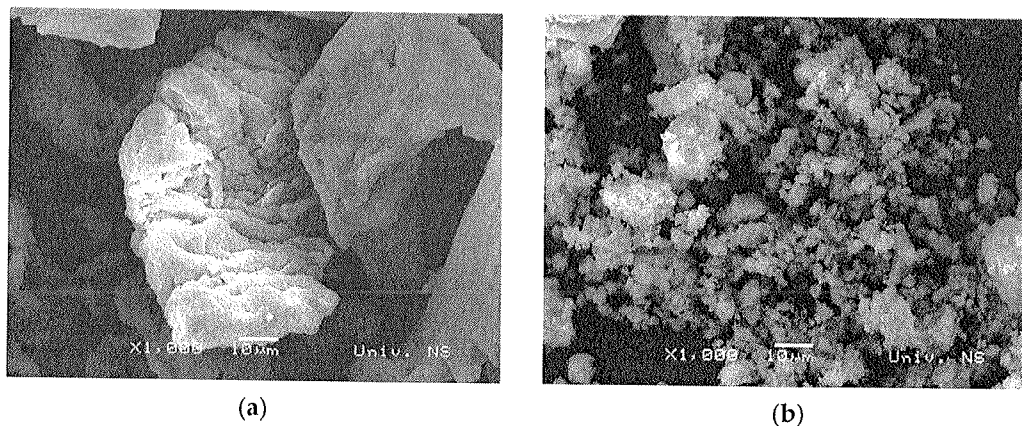


Figure 5. SEM micrographs of (a) commercial MgH_2 powder and (b) MgH_2 powder milled for 10 h.

SEM-EDS micrographs of composites $\text{MgH}_2\text{-V}$ show that vanadium layer particles are captured in MgH_2 powder (Figure 6). EDS maps of vanadium and magnesium prove that the dispersion of vanadium particles is very weak in magnesium hydride powder, but the size of vanadium particles increases with the increase of milling time. As shown by Bassetti et al. [25], the microstructure and morphology of $\text{MgH}_2\text{-Fe}$ nanocomposites can be changed by turning the ball milling energy and catalyst concentration, thus affecting the kinetic features of the hydride decomposition. The microstructure–sorption properties interplay was and still is the subject of extensive research [23,26,27]. Czujko et al. first demonstrated that microstructure changes occur in the first few minutes of mechanical activation [18].

3.2. Thermal and Kinetic Characterization of Materials

The TPD profiles of recombined hydrogen (H_2), H^+ , OH^- , and H_2O from 2V15 (a) and 5V15 (b) samples have been shown in Figure 7. Multiple peaks at different temperatures suggest the existence of differently bonded hydrogen atoms in the samples [22]. If a low quantity of catalyst is added, there is a pronounced recombination of hydrogen and oxygen to form H_2O , but also some OH^- ions are present too, possibly from the amorphous $\text{Mg}(\text{OH})_2$ phase [28], while in the 5V15 sample low-temperature peak originates from the recombination of H^+ to H_2 [29]. The existence of a low-temperature H_2 peak is due to smaller hydride particles.

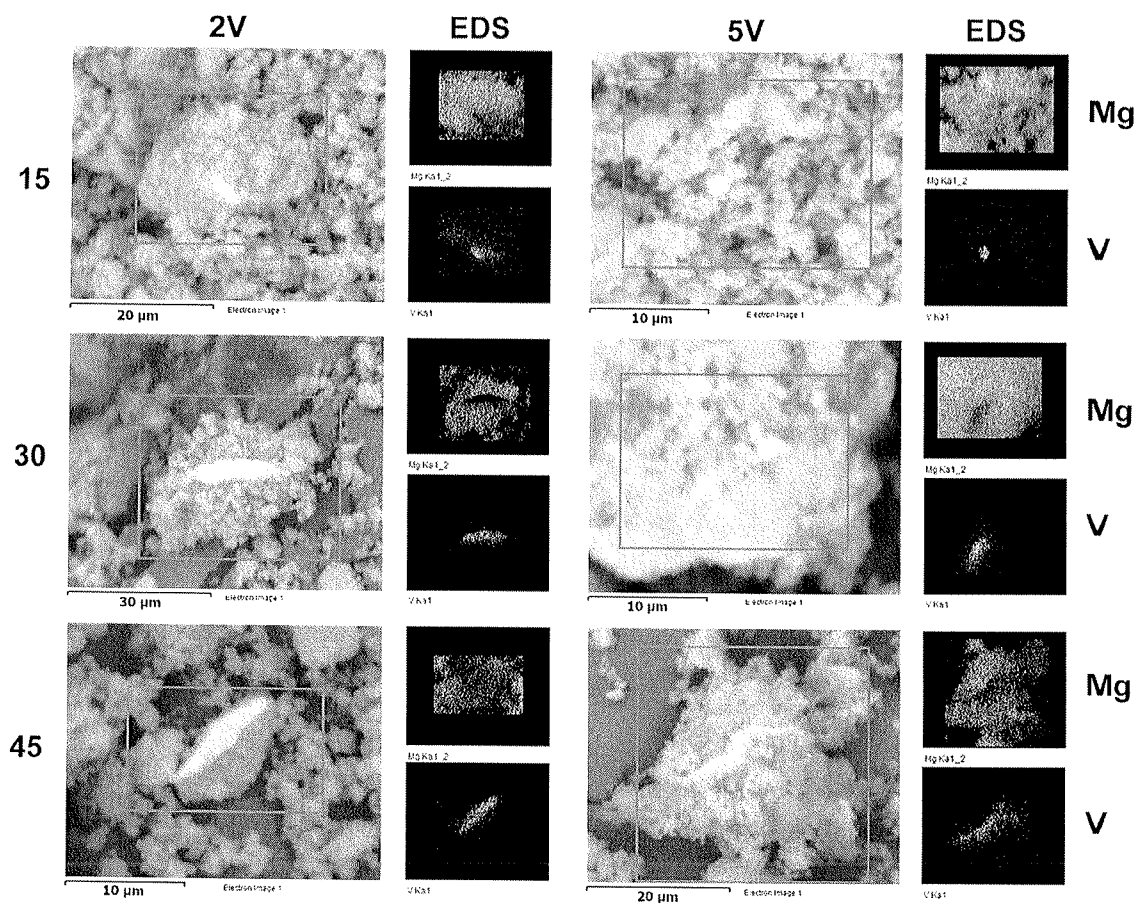


Figure 6. SEM micrographs and corresponding EDS Mg and V spectra of MgH_2 samples milled with 2 wt.% V (2V) and 5 wt.% V (5V) samples.

The DSC curve of commercial powder MgH_2 shows the endothermic desorption maximum of hydrogen at 454 °C (high temperature, HT), a value comparable to the literature [30]. As indicated earlier, a sharp symmetric HT maximum originates from desorption from rutile-structure (β) MgH_2 . The maximum of very low intensity (intermediate temperature, IT) is observed at about 350 °C, which is also expected [29]. IT peak is a consequence of surface-bound OH groups. Suppose the sample is exposed to the atmosphere and oxidation for a long time, a third, low temperature (LT) maximum [24,25] may occur, which originates from OH groups and water. It is observed that the hydrogen release temperature increases with increasing milling time, meaning that shorter milling times have an improving effect on the desorption properties of MgH_2 [18]. Figure 8a shows the thermograms obtained by DSC for 2V15, 2V30, and 2V45 samples. The endothermic desorption process in this composite significantly differs from the desorption from 5V samples. There is no desorption at low temperatures. Samples 2V15 and 2V30 composites are similar to pure milled hydride, with a wide maximum occurring at medium temperatures and an onset temperature of about 250 °C. For composites milled for 15 and 30 min, the maximum is shifted to temperatures above 454 °C. At temperatures of 450 °C and 460 °C, hydrogen is released from Mg(OH)_2 due to the oxidation of MgH_2 with oxygen from the air [31,32]. Figure 8b shows the thermograms obtained by DSC for 5V15, 5V30, and 5V45 samples. All three samples show a significantly different desorption profile than the commercial sample. The absence of desorption from medium temperatures is visible, but a pronounced LT peak appears at approximately 110 °C.

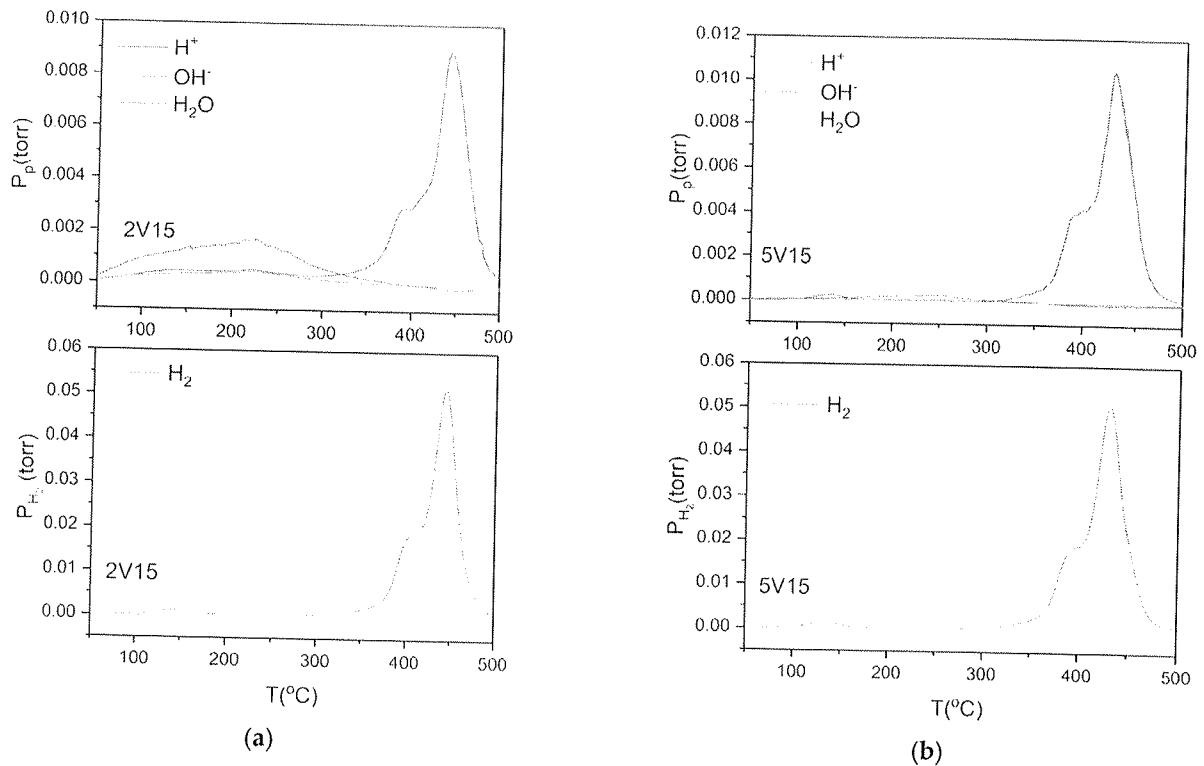


Figure 7. TPD profiles of MgH_2 samples milled with 2 wt.% V (a) and 5 wt.% V (b) samples.

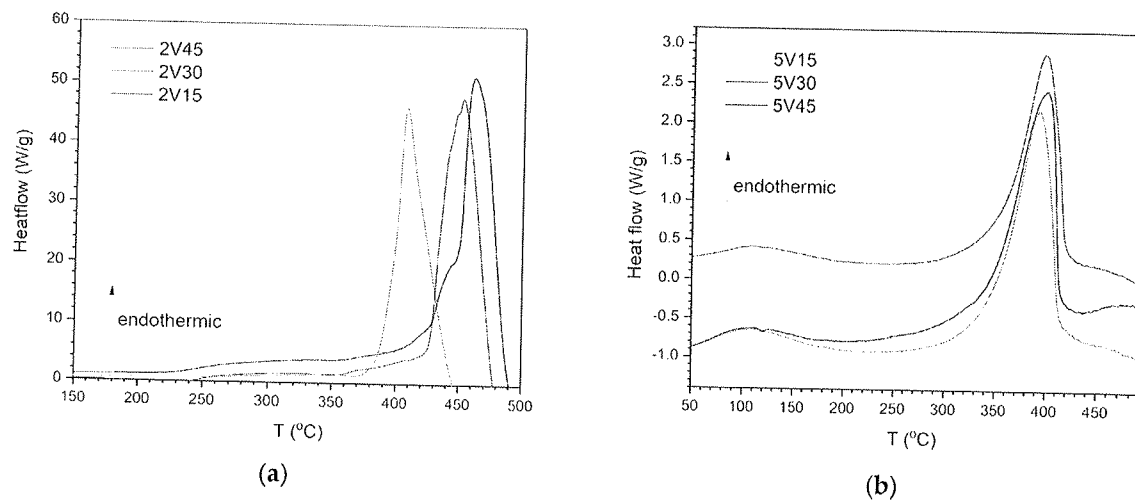


Figure 8. DSC curves MgH_2 samples milled with 2 wt.% V (a) and 5 wt.% V (b) samples.

For sample 5V15, the HT maximum occurs at 392 °C and corresponds to the release of hydrogen from $\beta - \text{MgH}_2$ (Table 3). The shift of the maximum by 62 °C is attributed to the reduction of the hydride particle size caused by mechanical milling. Similar behavior is shown by the other two composites milled for a longer time. The observed asymmetry of the DSC peaks could be explained by different PSDs and the presence of the gamma phase, as explained by Varin et al. [33].

Table 3. Positions of low temperature (LT), intermediate temperature (IT), high temperature (HT), and very high temperature (VHT). DSC maxima and corresponding apparent activation energies (Eapp). Estimated errors are given in parentheses.

Sample	LT (°C)	Eapp (kJ/mol)	IT (°C)	Eapp (kJ/mol)	HT (°C)	Eapp (kJ/mol)	VHT (°C)	Eapp (kJ/mol)
5V15	111.4(9)	4.91(7)	371.4(7)	27.7(3)	396.12(6)	90(1)	469.9(6)	60.3(2)
5V30	114.7(4)	5.21(7)	368.1(6)	25.9(3)	392.01(4)	78(1)	452.4(7)	61.5(7)
5V45	115.0(6)	3.38(6)	371.5(6)	32.3(3)	398.03(4)	82(1)	-	-
2V15	420(2)	59.5(4)	437.9(2)	224(2)	463.8(2)	108.9(7)	-	-
2V30	-	-	436.82(8)	250(2)	451.22(7)	96.9(5)	-	-
2V45	-	-	-	-	408.6(1)	106.7(7)	428.7(3)	158(1)

Section 3.1 shows no significant changes in microstructural morphology upon short-term milling since similar microstructure and morphology were obtained for pure MgH_2 [31]. This leads us to the conclusion that the addition of vanadium affects the thermal desorption of the material.

To investigate the desorption process in detail, different models of solid-state kinetics were used as implemented in the code developed in our group. The rate-limiting step of the desorption reaction was determined using the iso-conversional kinetic method due to better accuracy of obtained apparent activation energies [21,34]. As shown in Table 3, showing the received MgH_2 and milled one, for the same milling time [31], a decrease in apparent activation energies has been observed. It is obvious that the sorption kinetics is affected by material preparation because the reactivity of magnesium with hydrogen is strongly modified by changes in several surface parameters that govern the chemisorption, the dissociation of molecular hydrogen, and hydride nucleation [35,36]. Cui et al. [37] explained that desorption is affected significantly by the gas-solid interface. The first work by Isler [38] proposed that the reactivity of magnesium is determined by the free magnesium surface, while Vigeholm [39] indicates that surface nucleation and growth with a pressure-dependent concentration of nuclei is the mechanism of desorption. Therefore, the thermal decomposition of MgH_2 is a heterogeneous reaction. If there is an additive in milling blend, the sorption kinetics is also affected by the reaction at the Mg-Tm metal surface [11], but also the dispersion of Tm must be considered when defining a mechanism of desorption [12]. As shown in Table 3, adding 5 wt.% of vanadium leads to a significant decrease in apparent activation energies and temperature, 78 kJ/mol and 392 °C. An explanation of the change of mechanism is given. This value of apparent activation energy is close to the Mg-H bond-breaking energy suggesting that the breaking of this bond would be the rate-limiting step of the process [40]. The kinetic analysis done by Perejon et al. [40] on pure MgH_2 shows that the reaction of desorption follows the first-order kinetics, equivalent to an Avrami-Erofeev kinetic model with a corresponding coefficient equal to 3, suggesting that the mechanism of tridimensional growth of nuclei previously formed (A3) if desorption is done under pressure. Similar is obtained by other authors [4–10,12–16]. The additive change mechanism of desorption to Avrami Erofeev with parameter 4 (A4) is shown in Figure 9. Random nucleation is observed in all systems where defects are introduced [34].

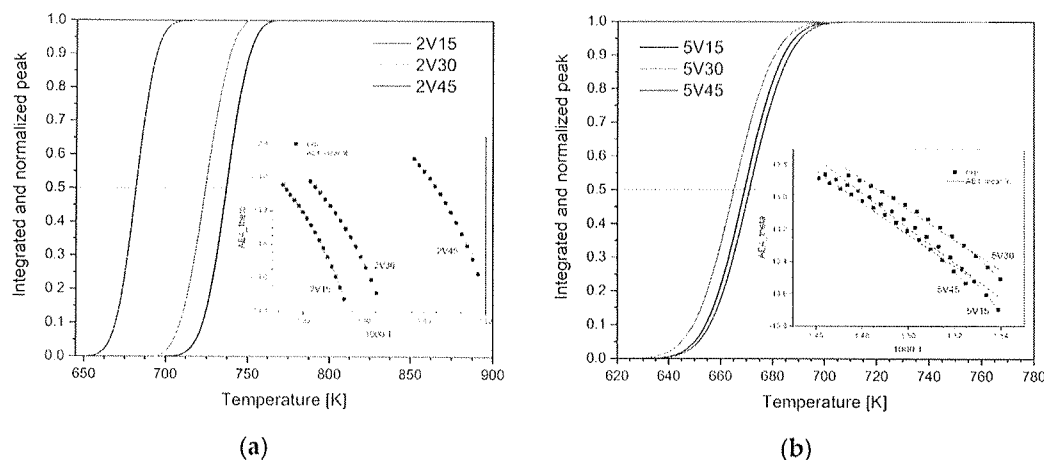


Figure 9. Temperature evolution of the reacted fraction (q) corresponding to MgH_2 -V decomposition, obtained by integration of HT- H_2 peaks for milling blends with 2 and 5 wt.% of vanadium and MgH_2 . Inserted figure: From $\ln g(0) = f(1/T)$, the best fit of experimental data is obtained for nucleation. (a) sample with 2 wt.% of V, (b) sample with 5 wt.% of V.

4. Conclusions

Using mechanochemical milling as a green synthesis method in an inert argon atmosphere, a magnesium hydride-vanadium composite was synthesized with a ball-to-powder mass ratio of 10:1, but different milling times from 15 to 45 min. As an additive, vanadium was added in 2 wt.% and 5 wt.%. The microstructure and morphology of the samples were examined and correlated with desorption properties monitored. The microstructure was monitored by X-ray diffraction analysis and infrared spectroscopy with Fourier transform, while morphology was examined by particle size distribution and scanning electron microscopy (SEM). The thermal behavior of milling blends was followed by TPD and DSC measurements. It was noticed that the presence of a dopant lowers the desorption temperature of hydrogen by several tens of degrees due to the catalytic action of vanadium. The best performance according to desorption temperature and apparent activation energy is expected for the 5V30 sample. Particle size distribution showed that even short milling times significantly reduce the particle size, which changes from a monomodal for as-received MgH_2 to a polymodal distribution for milling blends milled for 30 min. As this distribution follows the particle size distribution of pure, milled MgH_2 , we can assume that the decrease in desorption temperature is due to the added catalyst and its distribution in the bulk of the material. It has also been observed that, depending on the catalyst concentration, the temperature maximum shifts to the left or right of the value characteristic of pure hydride. TPD and FTIR measurements demonstrate the existence of OH^- ions and H_2O molecules. Those species give rise to intermediate and low-temperature desorption. Low-temperature desorption of H_2 is noticed and can be ascribed to a lower particle size of MgH_2 . It is shown that short milling times correspond to apparent activation energies of 70 kJ/mol, comparable to results obtained using longer milling times. Also, adding V using high-energy ball milling does not drastically influence the desorption temperature. This implies that it is better to use shorter milling times.

Author Contributions: Conceptualization, J.G.N.; Methodology, I.M. and V.A.; Software, N.N.; Investigation, Z.S., B.B., M.P., D.R. and N.F.; Writing—original draft, J.G.N. All authors have read and agreed to the published version of the manuscript.

Funding: This paper is supported by the Ministry of Science, Technological Development, and Innovation of the Republic of Serbia under Grants Nos. 451-03-47/2023-01/200017, and 451-03-47/2023-01/200175.

Data Availability Statement: Data is contained within the article The data presented in this study are available in this article.

Conflicts of Interest: The authors declare no conflict of interest.

References

- Bellosta von Colbe, J.; Ares, J.R.; Barale, J.; Baricco, M.; Buckley, C.; Capurso, G.; Gallandat, N.; Grant, D.M.; Guzik, M.N.; Jacob, I.; et al. Application of hydrides in hydrogen storage and compression: Achievements, outlook and perspectives. *Int. J. Hydrogen Energy* **2019**, *44*, 7780–7808. [CrossRef]
- Shao, H.; He, L.; Lin, H.; Li, H.W. Progress and Trends in Magnesium-Based Materials for Energy-Storage A Review. *Energy Technol.* **2017**, *6*, 445–458. [CrossRef]
- Andersson, J.; Grönkvist, S. Large-scale storage of hydrogen. *Int. J. Hydrogen Energy* **2019**, *44*, 11901–11919. [CrossRef]
- Sun, Z.; Lu, X.; Nyahuma, F.M.; Yan, M.; Xiao, J.; Zhang, S.L. Enhancing Hydrogen Storage Properties of MgH_2 by Transition Metals and Carbon Materials: A Brief Review. *Front. Chem.* **2020**, *8*, 552. [CrossRef] [PubMed]
- Grbović Novaković, J.; Novaković, N.; Kurko, S.; Milošević Govedarović, S.; Pantić, T.; Paskaš Mamula, B.; Batalović, K.; Radaković, J.; Shelyapina, M.; Skryabina, N.; et al. Influence of defects on Mg-based hydrides stability and hydrogen sorption behavior. *ChemPhysChem* **2019**, *20*, 1216–1247. [CrossRef]
- Liang, G.; Hout, I.; Boily, S.; Van Neste, A.; Schulz, R. Catalytic effect of transition metals on hydrogen sorption in nanocrystalline ball milled $MgH-Tm$ ($Tm = Ti, V, Mn, Fe$ and Ni) systems. *J. Alloys Compd.* **1999**, *292*, 247–252. [CrossRef]
- Liang, G.; Huot, J.; Boily, S.; Van Neste, A.; Schulz, R. Hydrogen storage properties of the mechanically milled MgH_2-V nanocomposite. *J. Alloys Compd.* **1999**, *291*, 291–299. [CrossRef]
- Gasan, H.; Celik, O.N.; Aydinbeyli, N.; Yaman, Y.M. Effect of V, Nb, Ti and graphite additions on the hydrogen desorption temperature of magnesium hydride. *Int. J. Hydrogen Energy* **2012**, *37*, 1912–1918. [CrossRef]
- Lu, Z.-Y.; Yu, H.-J.; Lu, X.; Song, M.-C.; Wu, F.-Y.; Zheng, J.-G.; Yuan, Z.-F.; Zhang, L.-T. Two-dimensional vanadium nanosheets as a remarkably effective catalyst for hydrogen storage in MgH_2 . *Rare Met.* **2021**, *40*, 3195–3204. [CrossRef]
- Hanad, N.; Ichikawa, T.; Fujii, H. Catalytic effect of nanoparticle 3d-transition metals on hydrogen storage properties in magnesium hydride MgH_2 prepared by mechanical milling. *J. Phys. Chem. B* **2005**, *109*, 7188–7194. [CrossRef]
- Paskaš Mamula, B.; Grbović Novaković, J.; Radisavljević, I.; Ivanović, N.; Novaković, N. Electronic structure and charge distribution topology of MgH_2 doped with 3d transition metals. *Int. J. Hydrogen Energy* **2014**, *39*, 5874–5887. [CrossRef]
- Montone, A.; Grbović Novaković, J.; Stamenković, L.J.; Pasquini, L.; Fiorini, A.L.; Bonetti, E.; Vittori Antisari, M. Desorption Behaviour in Nanostructured MgH_2-Co . *Mater. Sci. Forum* **2006**, *518*, 79–84. [CrossRef]
- Paik, B.; Walton, A.; Mann, V.; Book, D.; Jones, I.P.; Harris, I.R. Microstructure of ball milled MgH_2 powders upon hydrogen cycling: An electron microscopy study. *Int. J. Hydrogen Energy* **2010**, *35*, 9012–9020. [CrossRef]
- Montone, A.; Aurora, A.; Gattia, D.M.; Antisari, M.V. Microstructural and kinetic evolution of Fe doped MgH_2 during H_2 cycling. *Catalysts* **2012**, *2*, 400–411. [CrossRef]
- Wang, Y.; Wu, S.; Yu, H.; Gong, N.; Cao, Z.; Zhang, K. Hydrogen desorption/absorption kinetics of MgH_2 catalyzed with TiO_2 . *Adv. Mater. Res.* **2014**, *986–987*, 88–91.
- Hanada, N.; Ichikawa, T.; Hino, S.; Fujii, H. Remarkable improvement of hydrogen sorption kinetics in magnesium catalyzed with Nb_2O_5 . *J. Alloys Compd.* **2006**, *420*, 46–49. [CrossRef]
- Lototskyy, M.; Goh, J.; Davids, M.W.; Linkov, V.; Khotseng, L.; Ntsendwana, B.; Denys, R.; Yartys, V.A. Nanostructured hydrogen storage materials prepared by high-energy reactive ball milling of magnesium and ferrovandium. *Int. J. Hydrogen Energy* **2019**, *44*, 6687–6701. [CrossRef]
- Czujko, T.; Oleszek, E.E.; Szot, M. New Aspects of MgH_2 Morphological and Structural Changes during High-Energy Ball Milling. *Materials* **2020**, *13*, 4550. [CrossRef]
- Pantić, T.; Milanović, I.; Lukić, M.; Grbović Novaković, J.; Kurko, S.; Biliškov, N.; Milošević Govedarović, S. The influence of mechanical milling parameters on hydrogen desorption from MgH_2-WO_3 composites. *Int. J. Hydrogen Energy* **2020**, *45*, 7901–7911. [CrossRef]
- Milanović, I.; Milošević Govedarović, S.; Kurko, S.; Medić Ilić, M.; Rajnović, D.; Cvetković, S.; Grbović Novaković, J. Improving of hydrogen desorption kinetics of MgH_2 by $NaNH_2$ addition: Interplay between microstructure and chemical reaction. *Int. J. Hydrogen Energy* **2022**, *47*, 29858–29865. [CrossRef]
- Matović, L.J.; Kurko, S.; Rašković Lovre, Ž.; Vujasin, R.; Milanović, I.; Milošević, S.; Grbović Novaković, J. Assessment of changes in desorption mechanism of MgH_2 after ion bombardment induced destabilization. *Int. J. Hydrogen Energy* **2012**, *37*, 6727–6732. [CrossRef]
- Kurko, S.; Rašković, Ž.; Novaković, N.; Paskaš Mamula, B.; Jovanović, Z.; Bašćarević, Z.; Grbović Novaković, J.; Matović, L.J. Hydrogen storage properties of MgH_2 mechanically milled with alpha and beta SiC . *Int. J. Hydrogen Energy* **2011**, *36*, 549–554. [CrossRef]
- Varin, R.; Czujko, T.; Wronski, Z.S. *Nanomaterials for Hydrogen Storage*; Springer Science+Business Media: New York, NY, USA, 2009.

24. Wang, X.; Andrews, L. Infrared spectra of magnesium hydride molecules, complexes, and solid magnesium dihydride. *J. Phys. Chem. A* **2004**, *108*, 1151–1152. [CrossRef]
25. Bassetti, A.; Bonetti, E.; Pasquini, L.; Montone, A.; Grbović, J.; Vittori Antisari, M. Hydrogen desorption from ball milled MgH_2 catalyzed with Fe. *Eur. Phys. J. B* **2005**, *43*, 19–27. [CrossRef]
26. House, S.D.; Vajo, J.J.; Ren, C.; Rockett, A.A.; Robertson, I.M. Effect of ball-milling duration and dehydrogenation on the morphology, microstructure and catalyst dispersion in Ni-catalyzed MgH_2 hydrogen storage materials. *Acta Mater.* **2015**, *86*, 55–68. [CrossRef]
27. Polanski, M.; Bystrzycki, J.; Plocinski, T. The effect of milling conditions on microstructure and hydrogen absorption/desorption properties of magnesium hydride (MgH_2) without and with Cr_2O_3 nanoparticles. *Int. J. Hydrogen Energy* **2008**, *33*, 1859–1867. [CrossRef]
28. Baran, A.; Polański, M. Magnesium-Based Materials for Hydrogen Storage—A Scope Review. *Materials* **2020**, *13*, 3993. [CrossRef]
29. Leardini, F.; Ares, J.R.; Bodega, J.; Fernandes, J.F.; Ferrer, I.J.; Sanchez, C. Reaction pathways for hydrogen desorption from magnesium hydride/hydroxide composites: Bulk and interface effects. *Phys. Chem.* **2010**, *12*, 572–577. [CrossRef]
30. Milanović, I.; Milošević, S.; Rašković-Lovre, Ž.; Novaković, N.; Vujasin, R.; Matović, L.; Fernández, J.F.; Sánchez, C.; Novaković, J.G. Microstructure and hydrogen storage properties of MgH_2 - TiB_2 -SiC composites. *Ceram. Int.* **2013**, *39*, 4399–4405. [CrossRef]
31. Babić, B.; Prvulović, M.; Filipović, N.; Mravik, Ž.; Sekulić, Z.; Govedarozić, S.M.; Milanović, I. Hydrogen storage properties of MgH_2 -Tm: The Ni catalyst vs. mechanical milling. *Int. J. Hydrogen Energy* **2023**, in press. [CrossRef]
32. Martens, R.; Gentsch, H.; Freund, F. Hydrogen Release during the Thermal Decomposition of Magnesium Hydroxide to Magnesium Oxide. *J. Catal.* **1976**, *44*, 366–372. [CrossRef]
33. Varin, R.A.; Czujko, T.; Wronski, Z. Particle size, grain size and gamma- MgH_2 effects on the desorption properties of nanocrystalline commercial magnesium hydride processed by controlled mechanical milling. *Nanotechnology* **2006**, *17*, 3856–3865. [CrossRef]
34. Rašković Lovre, Ž.; Kurko, S.; Ivanović, N.; Fernandez, J.F.; Ares Fernandez, J.-R.; Šturm, S.; Mongstad, T.; Novaković, N.; Grbović Novaković, J. In-situ desorption of magnesium hydride irradiated and non-irradiated thin films: Relation to optical properties. *J. Alloys Compd.* **2017**, *695*, 2381–2388. [CrossRef]
35. Kurko, S.; Milanović, I.; Grbović Novaković, J.; Ivanović, N.; Novaković, N. Investigation of surface and near-surface effects on hydrogen desorption kinetics of MgH_2 . *Int. J. Hydrogen Energy* **2014**, *39*, 862–867. [CrossRef]
36. Novaković, N.; Matović, L.J.; Grbović Novaković, J.; Radisavljević, I.; Manasijević, M.; Ivanović, N. Ab Initio Calculations of MgH_2 , MgH_2 : Ti and MgH_2 :Co Compounds. *Int. J. Hydrogen Energy* **2010**, *35*, 598–608. [CrossRef]
37. Cui, J.; Liu, J.; Wang, H.; Ouyang, L.; Sun, D.; Zhu, M.; Yao, X. Mg-TM (TM: Ti, Nb, V, Co, Mo or Ni) core-shell like nanostructures: Synthesis, hydrogen storage performance and catalytic mechanism. *J. Mater. Chem. A* **2014**, *2*, 9645–9655. [CrossRef]
38. Isler, J. Etude Cinétique des Reactions d’Hydruration et de Deshydruration du Magnesium. Ph.D. Thesis, University of Dijon, Dijon, France, 1979.
39. Vigeholm, B.; Kjeler, J.; Larsen, B.; Pedersen, A.S. Formation and decomposition of magnesium hydride. *J. Less Common Met.* **1983**, *89*, 135–144. [CrossRef]
40. Perejon, A.; Sanchez-Jimenez, P.E.; Criado, J.M.; Perez-Maqueda, L.A. Magnesium hydride for energy storage applications: The kinetics of dehydrogenation under different working conditions. *J. Alloys Compd.* **2016**, *681*, 571–579. [CrossRef]

Disclaimer/Publisher’s Note: The statements, opinions and data contained in all publications are solely those of the individual author(s) and contributor(s) and not of MDPI and/or the editor(s). MDPI and/or the editor(s) disclaim responsibility for any injury to people or property resulting from any ideas, methods, instructions or products referred to in the content.